



HAL
open science

Ferrocene derivatives with planar chirality and their enantioseparation by liquid-phase techniques

Paola Peluso, Victor Mamane

► **To cite this version:**

Paola Peluso, Victor Mamane. Ferrocene derivatives with planar chirality and their enantioseparation by liquid-phase techniques. Electrophoresis, In press, 10.1002/elps.202200148 . hal-03769075

HAL Id: hal-03769075

<https://hal.science/hal-03769075v1>

Submitted on 5 Sep 2022

HAL is a multi-disciplinary open access archive for the deposit and dissemination of scientific research documents, whether they are published or not. The documents may come from teaching and research institutions in France or abroad, or from public or private research centers.

L'archive ouverte pluridisciplinaire **HAL**, est destinée au dépôt et à la diffusion de documents scientifiques de niveau recherche, publiés ou non, émanant des établissements d'enseignement et de recherche français ou étrangers, des laboratoires publics ou privés.

REVIEW

Ferrocene derivatives with planar chirality and their enantioseparation by liquid-phase techniques

Paola Peluso¹  | Victor Mamane²

¹Istituto di Chimica Biomolecolare ICB CNR, Sede secondaria di Sassari, Sassari, Italy

²Institut de Chimie de Strasbourg, UMR 7177, CNRS-Université de Strasbourg, Strasbourg, France

Correspondence

Paola Peluso, Istituto di Chimica Biomolecolare, Consiglio Nazionale delle Ricerche, Traversa La Crucca 3, Li Punti, 07100 Sassari, Italy.
Email: paola.peluso@cnr.it

Victor Mamane, Institut de Chimie de Strasbourg, Centre National de la Recherche Scientifique and Université de Strasbourg, 1 rue Blaise Pascal, 67008 Strasbourg Cedex, France.
Email: vmamane@unistra.fr

Color online: See the article online to view Figures 1, 2, 14, 17–20 and 23–28 in color.

Funding information

Consiglio Nazionale delle Ricerche; University of Strasbourg; Centre National de la Recherche Scientifique

Abstract

In the last decade, planar chiral ferrocenes have attracted a growing interest in several fields, particularly in asymmetric catalysis, medicinal chemistry, chiroptical spectroscopy and electrochemistry. In this frame, the access to pure or enriched enantiomers of planar chiral ferrocenes has become essential, relying on the availability of efficient asymmetric synthesis procedures and enantioseparation methods. Despite this, in enantioseparation science, these metallocenes were not comprehensively explored, and very few systematic analytical studies were reported in this field so far. On the other hand, enantioselective high-performance liquid chromatography has been frequently used by organic and organometallic chemists in order to measure the enantiomeric purity of planar chiral ferrocenes prepared by asymmetric synthesis. On these bases, this review aims to provide the reader with a comprehensive overview on the enantioseparation of planar chiral ferrocenes by discussing liquid-phase enantioseparation methods developed over time, integrating this main topic with the most relevant aspects of ferrocene chemistry. Thus, the main structural features of ferrocenes and the methods to model this class of metallocenes will be briefly summarized. In addition, planar chiral ferrocenes of applicative interest as well as the limits of asymmetric synthesis for the preparation of some classes of planar chiral ferrocenes will also be discussed with the aim to orient analytical scientists towards ‘hot topics’ and issues which are still open for accessing enantiomers of ferrocenes featured by planar chirality.

KEYWORDS

enantioseparation, ferrocenes, metallocenes, planar chirality, polysaccharide-based chiral stationary phases

Abbreviations: 2-PrOH, 2-propanol; B3LYP, Becke–3-parameter–Lee–Yang–Parr; B3PW91, Becke88, Perdew–Wang; CCSD, coupled cluster singles and doubles; CCSD(T), coupled cluster singles and doubles (triples); CD, cyclodextrin; CIP, Cahn–Ingold–Prelog; Cp, cyclopentadienyl; CSP, chiral stationary phase; DEA, diethylamine; def2-TZVP, default2-valence triple-zeta polarization; def2-TZVPP, default2-valence triple-zeta with two sets of polarization functions; DFT, density functional theory; *ee*, enantiomeric excess; EEO, enantiomer elution order; EtOH, ethanol; Fc, ferrocene; HB, hydrogen bond; IUPAC, International Union of Pure and Applied Chemistry; LANL2DZ, Los Alamos National Laboratory 2-double-z; MD, molecular dynamics; MeOH, methanol; MP, Møller–Plesset; PBE, Perdew–Burke–Ernzerhof; pinB, boron pinacolate; SCE, saturated calomel electrode; SFC, supercritical fluid chromatography; TEA, triethylamine; *V*, electrostatic potential; $V_{S,max}$, electrostatic potential maximum; $V_{S,min}$, electrostatic potential minimum; XB, halogen bond.

This is an open access article under the terms of the [Creative Commons Attribution](https://creativecommons.org/licenses/by/4.0/) License, which permits use, distribution and reproduction in any medium, provided the original work is properly cited.

© 2022 The Authors. *Electrophoresis* published by Wiley-VCH GmbH.

1 | INTRODUCTION

The concept of planar chirality was introduced in the mid-20th century [1] and subsequently discussed in a number of seminal papers focused on fundamentals of stereochemistry and stereoisomerism [2–5]. Later, in the International Union of Pure and Applied Chemistry (IUPAC) recommendations on the *Basic terminology of stereochemistry* [6], ‘planar chirality’ was defined as the *Term used by some authorities to refer to stereoisomerism resulting from the arrangement of out-of-plane groups with respect to a plane (chirality plane)*. On this basis, in planar chiral compounds such as cyclophanes, rigid alkenes and metallocenes, chirality arises from the different arrangements of groups located at both sides of a planar core. This feature induces a breaking of symmetry generating a chiral plane as the element of chirality (stereogenic unit) defining the stereochemical properties of this type of chiral compounds [7].

Metallocenes are organometallic coordination compounds in which one atom of a transition metal (iron, ruthenium, manganese, osmium, titanium and zirconium) is bonded to the face of two cyclopentadienyl [η^5 -(C₅H₅)] (Cp) ligands which lie in parallel planes [8]. In accord with the IUPAC recommendations on class names of organic compounds, the term ‘metallocene’ should not be used for analogues having rings other than Cp as ligand [8]. Planar chirality of metallocenes is related to their three-dimensional sandwich-like spatial arrangement where a transition metal is situated between two Cp ligands. Cp anions (Cp[−]) are achiral flat-shaped chemical species which upon disubstitution (R₁ ≠ R₂) presents two enantiotopic faces. Thus, π -coordination of the planar prochiral Cp[−] to a CpM⁺ (metal cyclopentadienyl cation) discriminates the two enantiotopic faces to induce planar chirality in the metallocene complexes. In other words, disubstitution (in 1,2- or 1,3-positions) of one of the Cp ligands of metallocenes generates a chiral plane (coloured in red, Figure 1) where the two sides of the plane are differently occupied.

The most prominent member of the metallocene family is ferrocene (M=Fe) (Fc) [9], the first sandwich complex discovered in early 1950s [10, 11] and structurally

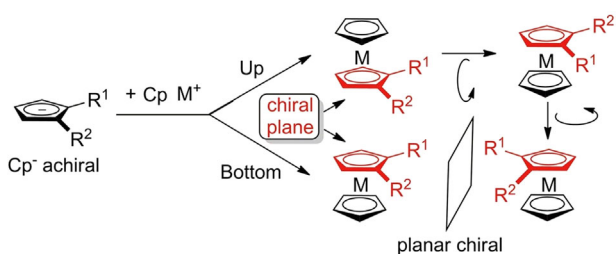


FIGURE 1 Planar chirality of metallocenes

elucidated shortly after [12–14]. Due to its high stability and similar reactivity to benzene, the ferrocene chemistry developed rapidly and until the late 1960s, a large number of planar chiral ferrocenes were reported, in particular by the group of Schlögl [15, 16].

The nomenclature rule proposed by Schlögl [17] to define the absolute configuration of planar chiral ferrocene compounds proceeds in three steps. First, considering the chiral plane, iron is assigned as the pilot atom (Figure 2) that is the linked atom being out of the chiral plane and with the highest priority based on the Cahn–Ingold–Prelog (CIP) priority rules [18]. Second, the chiral plane is observed from the top, thus positioning the iron atom beneath the plane. Third, the two substituents on the Cp are classified according to CIP priority rules: if the relative orientation from the first-priority substituent to the second one is clockwise, the molecule is assigned as an (*R*)-stereoisomer; if it is counterclockwise, the molecule is assigned as an (*S*)-stereoisomer (Figure 2). Because central and planar chirality may be both present in ferrocene derivatives, the planar chirality of ferrocene is usually differentiated by adding the letter ‘p’ (R_p and S_p or pR and pS) or the acronym ‘Fc’ (R_{Fc} or S_{Fc}) to specify that the nomenclature corresponds to the planar chirality. Actually, there are other (*R*)/(*S*)-nomenclature rules to define the absolute configurations in planar chiral iron complexes which possess π -ligands [19]. However, the nomenclature proposed by Schlögl remains the most used in planar chiral ferrocene chemistry.

It is worth mentioning that, in principle, *P* and *M* helical enantiomeric conformations (*P* [plus] and *M* [minus], respectively, represent the right- and left-handed helicities) are present in the 1,*n*'-disubstituted ferrocenes (Figure 3). However, they are interconvertible based on a torsional twist about the Cp(centroid)–Fe–Cp(centroid) axis [20]. Thus, 1,*n*'-disubstituted ferrocenes are not chiral unless electronic or steric constraints impede the torsional twist about the Cp–Fe–Cp axis.

Over time, the main field of application of planar chiral ferrocenes has been asymmetric catalysis. It was in the early 1990s that the usefulness of chiral

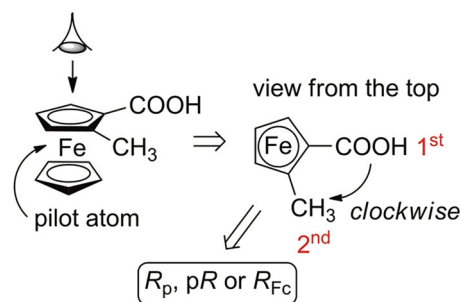


FIGURE 2 Absolute configuration of planar chiral ferrocenes

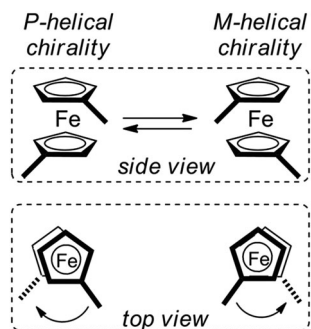


FIGURE 3 Side and top views of *P* and *M* helical chirality of the ferrocene moiety of 1,*n'*-disubstituted ferrocenes

ferrocenylphosphines in asymmetric catalysis was recognized [21, 22], and an impressive number of planar chiral ferrocenes were produced on the basis of diastereoselective methodologies implying the use of different chiral auxiliaries [23–25]. The majority of chiral ferrocene ligands available so far have both central and planar chirality [21]. In some cases, both chiral elements proved to act synergistically (matched combination), providing high asymmetric induction [26, 27]. On the other hand, there are a growing number of ferrocene ligands with only planar chirality that provide excellent enantioselectivities [28, 29]. In the last decade, planar chiral ferrocenes have been attracting a growing interest beyond asymmetric synthesis, finding application in other fields such as medicinal chemistry [30], chiroptical spectroscopy [31–33] and electrochemistry [34, 35].

In 1970, Ugi et al. reported a pioneering work on the diastereoselective synthesis of 1,2-disubstituted ferrocene derivatives starting from enantiopure *N,N*-dimethyl-1-ferrocenylethylamine [36]. In addition, methodologies based on the direct enantioselective synthesis from prochiral ferrocenes have been developed [37, 38]. Liquid-phase enantioseparation can also be used to access pure or enriched enantiomers of planar chiral ferrocenes [39]. A reason which makes the availability of efficient enantioseparation methods urgent is that, in some cases, asymmetric synthesis procedures for accessing enantiomerically enriched ferrocenes not always provide products with satisfactory enantiomeric purity [40–42]. Moreover, for a long time the preparation of pure enantiomers of certain planar chiral ferrocenes, for instance those containing a pyridine core, required diastereomeric resolution or enantioselective high-performance liquid chromatography (HPLC) separation [38, 43]. However, despite the growing interest in planar chiral ferrocenes containing only a chiral plane as a stereogenic unit (Figure 4A, B), the enantioseparation of this type of compounds was not comprehensively explored, and very few systematic analytical studies were reported so far [44–48]. On the other

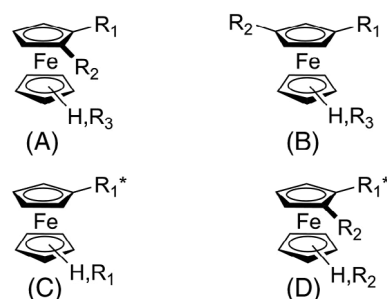


FIGURE 4 Chiral ferrocene motifs studied in enantioseparation science (R_1^* = chiral framework): planar chiral ferrocenes containing only a chiral plane as a stereogenic unit (A,B); chiral ferrocenes featured by a single chiral centre as a stereogenic unit (C); planar chiral ferrocenes featured by both central and planar chirality (D)

hand, enantioselective HPLC has been frequently used in organic and organometallic chemistry studies in order to measure the enantiomeric purity of planar chiral ferrocenes prepared by asymmetric synthesis. In these cases, the chromatographic analyses have been in general performed under normal phase conditions, this trend being likely due to the fact that non-analytical scientists are more familiar with this elution mode compared to polar organic and reversed-phase modes. Over time, several methods were also developed for the enantioseparation of chiral ferrocenes featured by a single chiral centre as a stereogenic unit (Figure 4C) [49–53] or by both central and planar chirality (Figure 4D) [48].

Given this context and aiming to provide the reader with a comprehensive overview of the field, this review describes liquid-phase enantioseparation of planar chiral ferrocenes, integrating this main topic with other relevant aspects of ferrocene chemistry. For this purpose, in the first part, introductory topics will be presented: (a) structural features of ferrocenes (Section 1.1); (b) the main computation tools currently available to model ferrocene structures will also be briefly summarized (Section 1.2). In this regard, it is worth mentioning that in modern enantioseparation science, integrating experimental and theoretical data has proven to be a useful tool to understand the enantioseparation mechanisms at molecular level. Approaches to model HPLC enantioseparation of planar chiral ferrocenes were not reported until very recently [45]; (c) applications which justify the growing interest in planar chiral ferrocene chemistry (Section 2.1); (d) the main asymmetric syntheses available to access enantiomerically enriched planar chiral ferrocenes, highlighting advances and limitations of the synthetic approaches (Section 2.2).

In the second part (Section 3), with the aim to profile the historical advancement of the field as well as the state-of-the-art of liquid-phase enantioseparations of planar chiral ferrocenes, methods, techniques and

chiral stationary phases (CSPs) used in this field over time will be overviewed, highlighting the relationships between the structural features of the analytes and the chromatographic outcomes.

1.1 | General features of the ferrocene structure

Besides the possibility of being chiral, ferrocene possesses exceptional structural and electronic characteristics [9]. With an iron centre that has the saturated electronic structure of krypton, ferrocene is thermally stable up to 400°C, tolerant to light, oxygen and moisture. It has good solubility in all common organic solvents and is easily functionalized by common procedures. The Cp rings in ferrocenes carry a partial negative charge; thus, they have electron donor properties and may undergo electrophilic substitution [54]. Owing to these features, over time ferrocene derivatives have found application in several fields such as catalysis [22], material sciences [55–58] and medicinal chemistry [59–61]. Indeed, ferrocene presents low toxicity that allows its use as a bioisostere of aryl and heteroaryl groups [30, 62, 63]. Moreover, ferrocene possesses mild and reversible oxidation around +0.4 V versus saturated calomel electrode. Thus, the ferrocenium/ferrocene system (Fc^+/Fc) is a versatile redox couple which was shown to be suitable for the preparation of switchable functional systems [64].

An interesting structural feature of ferrocene is that the inter-ring distance between the two Cp rings is about 3.3 Å, which is suitable for hydrogen bonding (HB) [20], and in principle for other noncovalent interactions, between attached groups on the two Cp rings [65]. Recently, by integrating experimental and computational analyses, it was demonstrated that in chiral ferrocenes, featured by central and/or planar chirality, intra- and intermolecular HBs involving neighbouring groups may affect the conformational properties of the ferrocene system in terms of eclipsed ($D5h$) or staggered ($D5d$) structures of the two Cp rings (Figure S1), as well as their chiroptical responses [33, 66]. In this regard, the eclipsed conformation is reported to be the most stable one at room temperature for ferrocene in solution [67, 68], and for mono-substituted ferrocenes [68, 69]. Density functional theory (DFT) computations showed that the interconversion barrier between equivalent eclipsed conformers (stable minima) and the staggered conformers (saddle points) is small in ferrocene [66, 70]. The $D5d$ – $D5h$ barrier to internal rotation of the ligand rings was estimated at 0.9 kcal/mol [71]. Otherwise, in some cases, the staggered conformation was shown to be favoured by intermolecular interactions in the crystalline state [72].

1.2 | Basic concepts of ferrocene modelling

In the last few years, the integration of computational and experimental analysis has been developing as a pivotal tool to disclose enantioselective recognition mechanisms at molecular level [73–75]. In this field, the selection of the proper combination of method, functional and basis set for geometry optimization and calculations of molecular properties of the selected structures is essential in order to obtain reliable theoretical information. However, in general this choice is guided by the need to find the best compromise between calculation reliability and computational time required for performing the calculations with a given method. The coupled cluster singles and doubles (CCSD) and triples (CCSD(T)) methods are considered the ‘gold standard’ quantum chemical methods, but with a computational time cost which is not negligible. Early Hartree–Fock calculations for geometry optimization of ferrocene were performed in the 1980s by Lüthi et al. providing a metal–ligand distance of 1.88 Å [76], in poor agreement with the experimental value of 1.66 Å [71, 77]. In 1996, Koch, Jørgensen and Helgaker performed CCSD and CCSD(T) calculations on (staggered) ferrocene and obtained metal–ligand distances of 1.672 and 1.660 Å, respectively, in close agreement with the experimental data [78]. In 2006, Coriani et al. compared different functionals to model the equilibrium structure of ferrocene using the Møller–Plesset (MP2), CCSD and CCSD(T) models [70]. Although the MP2 model failed, the CCSD(T) results agreed very well with the experimental bond lengths. Moreover, the comparison with DFT results indicated that the Becke–Lee–Yang–Parr B3LYP model yields the best results in comparison to both experimental data and CCSD(T) calculations. In particular, B3LYP provided an error of about 0.02 Å for the metal–ligand distance and smaller errors for the cyclopentadienyl rings (up to 0.01 Å). Otherwise, the Becke–Perdew BP86 method afforded a metal–carbon distance only 0.001 Å off experimental values, but rather large deviations in the cyclopentadienyl C–C and C–H bonds. Full geometry optimization of ferrocenes was also performed by using the functional B3LYP and the m6-31G(d) as basis set that incorporates necessary diffuse d-type functions for the first-row transition metals such as Fe, thus exhibiting better performances than the conventional 6-31G(d) basis set for the iron atom in ferrocene [79, 80]. Latouche et al. tested different combinations of functionals and basis sets for metallocenes including ferrocene [81]. Although the Perdew–Burke–Ernzerhof (PBE0) functional underestimated the Fe–Cp distance, the best agreement for this distance was obtained at the Coulomb-attenuating method–B3LYP and B3PW91 levels. On this basis, recently Barone et al. used the

hybrid functional B3PW91 with the def2TZVP as basis set for DFT geometry optimization and frequency calculations of substituted ferrocenes [32, 33, 66]. Yáñez-S et al. reported the full geometry optimization of the ground state of the 2-ferrocenyl-1,8-naphthyridine at the B3LYP/6-31++G(d) level of theory, and the LANL2DZ basis set with the effective core potential was used to describe Fe [82]. The comparison of calculated and crystallographic structures showed that both geometries (eclipsed) were nearly equal with slight deviation in the cyclopentadienyl rings and in the naphthyridine region [82]. A similar computational method (B3LYP/LANL2DZ(Fe,I)/6-31G(d)) was recently used by Erb et al. for geometry optimization and calculations of molecular properties of a series of *N,N*-dialkylferrocenesulfonamides [83].

In 2011, Bogdanović and Novaković evaluated the frequency of occurrence of the ferrocene dimer in crystals reported in the Cambridge Structural Databank [84], finding that 46.8% of ferrocene derivative crystals contained a dimer. Vargas-Caamal et al. showed by computations that dispersion is the major contribution to stabilize a metallocene dimer [85]. In this study, final equilibrium geometries were calculated at PBE/def2-TZVP and PBE-D2/def2-TZVP levels, the latter approach including the D2 version of Grimme's dispersion corrections [86]. Indeed, DFT methods have shown fundamental problems to describe properly dispersion forces that require suitable methods or corrected DFT methods for a proper description. On the other hand, the impact of dispersion on geometry optimization and calculation of some properties of molecules in their unbound state may be low. Recently, our groups optimized the geometry of halogenated ferrocenes **1–5** (Table S1), in their unperturbed isolated state in the vacuum, at DFT level of theory, by using the B3LYP functional with [87] and without [46] D3 dispersion correction, and the Ahlrichs-type triple- ζ valence def2-TZVPP basis set. Under these conditions, the local maxima of the electrostatic potential ($V_{S,max}$) values were calculated on the 0.002 au isodensity surface. As expected, dispersion corrections provided less positive $V_{S,max}$ values and smaller variations as the structure of the ferrocene changes. However, the variation of the relative magnitudes, normalized with respect to the 1-chloro-2-iodoferrocene (**1**), revealed that the obtained trends for the series **1–5** are very similar in both cases.

2 | PLANAR CHIRAL FERROCENES

2.1 | Recent applications of planar chiral ferrocenes

Among various applications of ferrocenes [62, 88, 89], asymmetric catalysis is by far the domain where planar

chirality of substituted ferrocenes was mostly employed. Starting from the 1990s, a huge number of planar chiral ferrocenes were developed as ligands for asymmetric catalysis. Among them, well-known P,N- and P,P-ligands such as Fc-Phox (**6**) [90], Josiphos (**7**) [91], Taniaphos (**8**) [92], Walphos (**9**) [93] (Figure S2) have been applied with remarkable asymmetric efficiency, even at industrial level for the production of enantiopure chemicals [94, 95]. Multiple substitution patterns have been used in the preparation of planar chiral ferrocene catalysts, including 1,2-disubstituted, 1,1',2-trisubstituted, 1,1',2,2'-tetrasubstituted, polysubstituted and heterocyclic ferrocenes as well as bisferrocenes [21]. As several excellent reviews have been published in this field over time [21, 22, 54, 96], we will report herein only a selection of very recent planar chiral ferrocenes used as organocatalysts or ligands in metal-catalysed reactions, highlighting the motifs which have been attracting attention of chemists in the last few years in order to expand the scope of ferrocenyl ligands and catalysts [22].

Ferrocene has been considered a privileged framework for the construction of chiral organocatalysts [97]. Very recently, planar chiral catalysts **10–12** (Figure S3), featuring ferrocene-fused nitrogen heterocycles, were developed as systems where the ferrocene backbone provides planar chirality, whereas the heterocyclic moiety maintains its nucleophilic and basic character [98–105]. Although chiral ferrocenyl catalysts were developed for a long time in asymmetric noncovalent organocatalysis [97], it is not until the last 2 years that our groups reported the first examples of halogen bond (XB)-based chiral ferrocenyl catalysts [87, 106]. However, only 6% *ee* was obtained with the planar chiral bis-triazolium catalyst **13** in an aza-Diels-Alder reaction (Figure S4) [106].

Several examples of planar chiral ferrocenyl phosphines such as monophosphines **14–16** were used as ligands in metal-catalysed reactions, which were recently reported (Figure S5) [107–109]. Interestingly, Echavarren et al. also reported a series of unusual 1,3-disubstituted ferrocenyl monophosphines **16** as ligands in gold(I)-catalysed reactions [109]. Indeed, 1,2-disubstitution in planar chiral ferrocenes remains a privileged motif, which is prone to function for metal coordination, also through chelating effect. Moreover, most ferrocene ligands and catalysts reported so far combine planar and central chirality, this type of systems affording very positive results in asymmetric catalysis. This trend has also continued in recent years as shown with most recent ferrocenyl monophosphines [110, 111], phosphine phosphoramidite ligands [112], diphosphines [113] and tridentate PNP ligands [114] developed for metal-catalysis.

Although the impact of planar chirality is not obvious in medicinal chemistry and material science, planar chiral ferrocenes have found important interest also in these

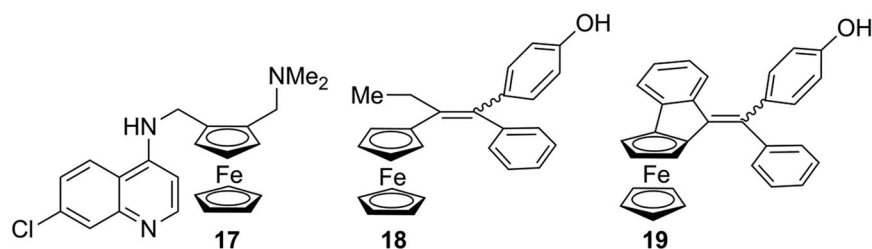


FIGURE 5 Structures of ferroquine (**17**), ferrocifen (**18**) and planar chiral derivative **19**

fields. Drugs based on the ferrocenyl moiety are attractive because of their good stability, nontoxicity and the ability of ferrocene to generate reactive oxygen species that can induce apoptosis [115]. One of the first described planar chiral ferrocenes with important biological activity is ferroquine **17** (Figure 5), an analogue of the well-known antimalarial chloroquine [116, 117]. The antimalarial and cell antiproliferative activities of both enantiomers were compared, and no significant differences were found [118]. Afterwards, many other ferroquine analogues were studied for their antimalarial and antiplasmodial activities [119, 120]. Achiral ferrocifen **18** (Figure 5) represents another important class of biologically active compounds initially developed for their structural analogy to tamoxifen, an anti-tumour drug used in breast cancer therapy [121]. A large number of ferrocifen derivatives with remarkable structural and mechanistic diversity are currently available [61], but only a few being planar chiral [122, 123]. More recently, Guiry et al. described the synthesis of enantiopure analogue **19** of ferrocifen (Figure 5). The biological evaluation of both enantiomers of **19** revealed moderate anticancer activities on breast cancer cells with some difference between the enantiomers [124].

A number of other polycyclic and heterocyclic structures based on planar chiral ferrocenes with interesting biological activities such as compounds **20–26** were also reported these last years, which are depicted in Figure S6 [125–132].

Electrochemical and photophysical properties of ferrocenes combined with planar chirality have resulted in many applications in material sciences. In this field, 1,3-disubstituted planar chiral ferrocenes were used for the elaboration of optically active liquid-crystalline polymers [133, 134]. A series of chiral ferrocenic chromophores were also studied for their ability to give non-linear optic responses in solution and in the solid state [135–138]. Interestingly, the two planar chiral ferrocenic compounds **27** and **28** were reported to act as electrochemical sensors of chiral dicarboxylates (Figure 6). Although with **27** the combination of central and planar chirality was necessary to obtain good sensing properties [35], interesting results were obtained with the polytopic ligand **28** carrying only planar chirality [139]. Conversely, in a more recent work, chiral ferrocenes of the general structure **29** (Figure 6) were

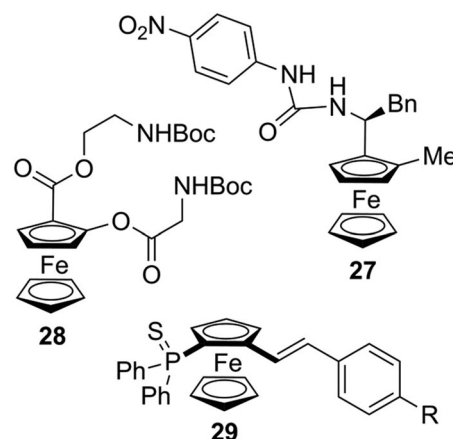


FIGURE 6 Planar chiral ferrocenes studied in the field of electrochemical sensing

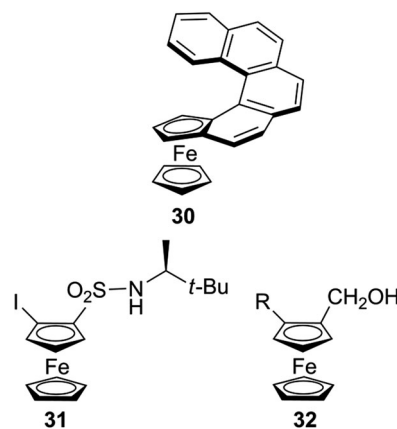


FIGURE 7 Planar chiral ferrocenes studied as test probes for their chiroptical properties

efficiently enantiodifferentiated on chiral polythiophene inherently chiral electrodes [34].

In the frame of studies on helical chiral molecules that show strong chiroptical properties, the (R_p)-enantiomer of ferrocene **30** (Figure 7) showed very interesting chiroptical properties, highlighted by exceptional optical rotation value ($[\alpha]_D^{20} = +3240$) and strong circular dichroism signals [31]. In particular, this planar chiral ferrocene showed additional helical chirality, as a result of a high distortion of the planarity, generating a significant transfer of chirality from the planar chiral ferrocene moiety

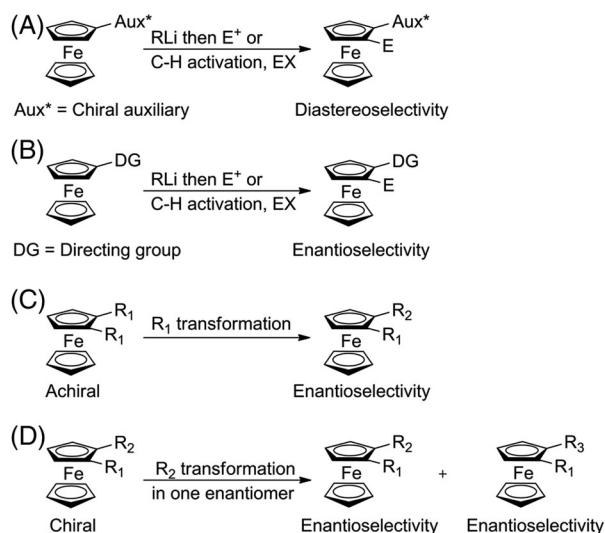


FIGURE 8 Main approaches for the stereoselective synthesis of planar chiral ferrocenes: diastereoselective methods (A); enantioselective methods (B); desymmetrization of achiral ferrocenes (C); kinetic resolution of chiral ferrocenes (D)

to the helical *ortho*-condensed aromatic system [31]. Very recently, experimental ECD and VCD spectra of compounds **31** and **32**, used as test probes, were recorded and studied with the assistance of quantum chemical computations, which allowed for an unambiguous analysis of the different structural factors that may impact the overall spectroscopic features [32, 33] (Figure 7).

2.2 | Preparation of planar chiral ferrocenes: asymmetric synthesis versus enantioseparation

Since the seminal work of Ugi and the revival observed in the early 1990s, three main strategies for the asymmetric synthesis of planar chiral ferrocenes were developed in the literature based (a) on kinetic resolution [140] and desymmetrization methods, (b) on diastereoselective and (c) on enantioselective functionalizations relying on the use of lithiation/electrophilic quenching sequence [25] or metal-catalysed C–H activation [141]. Diastereoselective methods (Figure 8A) are by far the most employed ones, but the use of chiral auxiliaries is a limiting factor. Indeed, this method involves additional steps to introduce and remove the required substituent. This is the reason why enantioselective methods (Figure 8B) are nowadays more and more targeted. However, the enantiomeric purity of the final products is not as high as the ones obtained through diastereoselective methods. Other very attractive but less explored methods are those based on desymmetrization of achiral ferrocenes (Figure 8C) and on kinetic resolution of chiral ferrocenes (Figure 8D).

Consequently, the number of syntheses of planar chiral ferrocenes is extremely large. However, the search for methods to efficiently obtain pure enantiomers cannot be limited to asymmetric syntheses for the different reasons listed as follows:

- Except for some well-established diastereoselective methods, it is very rare that the planar chiral ferrocenes are obtained as single enantiomers. Even when very efficient methods are employed, enantiomeric purity over 95% is achieved only in specific cases but most often, depending of the nature of the substituents, it is not sufficiently high.
- Most of the reported asymmetric syntheses give access to only one of both enantiomers.
- There are still some planar chiral ferrocene structures lacking efficient asymmetric synthesis.

These reasons thus justify that more attention should be given to the development of efficient enantioseparation methods. In the following, we will give selected examples illustrating some limitations of asymmetric synthesis for accessing chiral ferrocenes with high enantiomeric purity (Figures 9 and 10):

- An enantioselective C–H activation/annulation strategy for the synthesis of ferrocene-fused heterocycles **33** was recently reported [142]. The Rh-catalysed reaction between ferrocenecarboxamides and internal alkynes afforded the desired compounds, providing high enantiomeric excesses (*ees*) only when alkyl/aryl nonsymmetric alkynes were used. In contrast, by using the symmetric dialkyl alkyne hex-3-yne as reagent, a low *ee* of 41% was obtained.
- A Pt-catalysed reaction was used for the synthesis of planar-chiral naphthalene-fused ferrocenes **34** [143]. Although the non-substituted derivative ($R = H$) was obtained with 97% *ee*, only a low *ee* of 36% was achieved for the ester-substituted compound ($R = CO_2Et$). A similar strategy was also used for the synthesis of azepine-fused ferrocene derivatives **35** but the *ees* were generally moderate [144].
- The direct Pd-catalysed asymmetric C–H acylation of 1-dimethylaminomethylferrocene generated compounds **36** with high *ees* for insertion of arylketones ($R = Ar$), but a lower *ee* was obtained in the case of methylketone ($R = Me$) [40].
- Several publications reported efficient C–H functionalization methods for the synthesis of planar chiral ferrocenes that generally resulted in moderate *ees* [145]. The enantioselective alkylation of amidoferrocene with diethylmalonate generated compounds **37** with *ees* between 64% and 88% [146].

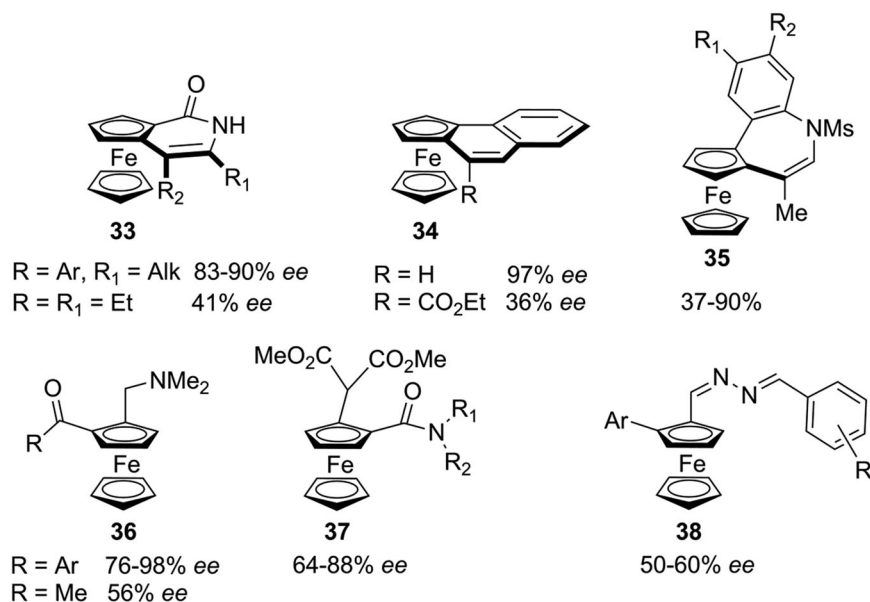


FIGURE 9 Planar chiral ferrocenes obtained with low to moderate *ees*

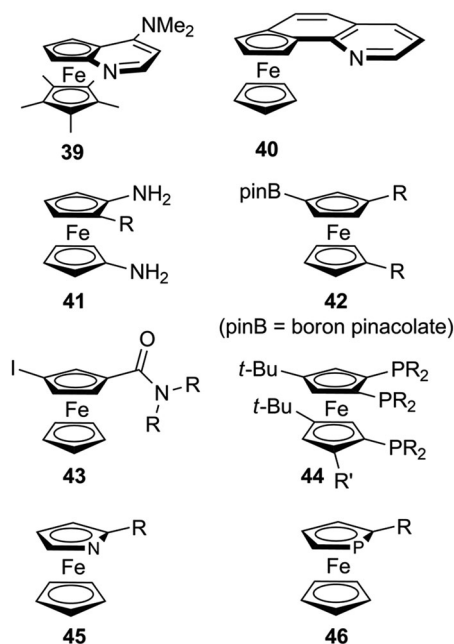


FIGURE 10 Planar chiral ferrocenes and derivatives with limited availability in their enantiopure forms

5. A Pd/chiral ligand system was used recently for the double C–H activation of an azine-based ferrocene to provide heteroaryl functionalized ferrocenes **38** with *ee* in the range 50%–60% [147].
6. As mentioned earlier (see Figure S3), the planar chiral aminopyridine derivatives based on the ferrocene ligands developed by Fu have shown excellent enantioselectivity in a wide range of asymmetric reactions [100, 148]. Interestingly, both enantiomers of **39** could be enantioseparated by HPLC [28]. In two more recent publications by the group of Ogasawara and Yoshida,

the asymmetric synthesis of **39** and analogues was realized but only the (*S*_{FC}) enantiomers could be prepared [43, 99]. More extended benzoquinoline derivative **40** was also prepared for catalysis purposes and, again, only the (*S*_{FC}) enantiomer was prepared by asymmetric synthesis [149].

7. The asymmetric synthesis of some relevant planar chiral ferrocene derivatives, such as those functionalized in 1,3-positions and in both Cp rings, are currently seldom explored in the literature. Planar-chiral 1,1'-diaminoferrocenes **41** were recently prepared as racemates, which are key substrates for the synthesis of chiral *N*-heterocyclic carbenes and tetrylene analogues [150]. On the other hand, the synthesis of enantioenriched or enantiopure 1,3-disubstituted ferrocenes is much more difficult compared to the 1,2-disubstituted one, because the strategies relying on directed functionalization cannot be applied. For instance, enantioenriched and enantiopure borylated planar-chiral ferrocenes, which represent important building blocks for the synthesis of more functionalized chiral compounds, were described for accessing 1,2-disubstituted derivatives [42, 151], whereas no asymmetric method is currently available for 1,3-disubstituted ferrocenes **42** [152]. Analogously, several asymmetric methods are available for the synthesis of 1-iodo-2-amidoferrocenes, but no direct methods were described for the synthesis of enantioenriched or enantiopure 1,3-disubstituted derivatives **43**, for which an efficient racemic synthesis was described [153], exclusively.
8. In the last decade, the Hierso group reported several planar chiral polyphosphine derivatives **44** as efficient ligands in coordination chemistry [154–156], but

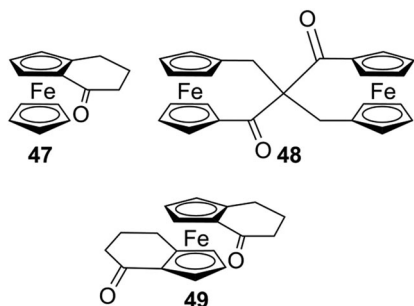


FIGURE 11 Structures of ferrocene derivatives 47–49

because of their structural complexity, no asymmetric synthesis was explored.

- Two heteroatom-containing ferrocenes, namely azaferrocene **45** and phosphoferrocene **46**, represent important analogues of ferrocene with reported applications in asymmetric catalysis [157]. These derivatives are planar chiral when only one position of the heterocyclic ring is functionalized and several derivatives could be enantioseparated by HPLC [148, 158]. However, their preparation in enantiopure forms through asymmetric synthesis remained scarce. The asymmetric synthesis of planar chiral azaferrocenes relied either on the *n*-BuLi/sparteine strategy to deprotometallate enantioselectively one α -position [159, 160], or on the Kagan's chiral sulfoxide strategy [161, 162]. Enantiopure phosphoferrocenes were generally obtained by a prior synthesis of chiral phospholides [163, 164], and their direct enantioselective formation was reported only in one instance [165].

The examples mentioned before contributed to profile a scenario where liquid-phase enantioseparation still may play a pivotal role for accessing planar chiral ferrocene in enantiopure or enriched form. Despite that, so far limited attention has been devoted to this issue by scientists operating in the field of enantioseparation science.

3 | ENANTIOSEPARATION OF PLANAR CHIRAL FERROCENES

In the late 1950s, most methods for obtaining enantiopure chiral ferrocenes relied on chemical resolution through diastereoselective crystallization. In 1959, Thomson reported the resolution of the first chiral ferrocene derivative, namely, ferrocenocyclohexenone **47** (Figure 11), by diastereomeric crystallization [166].

Later, the first chromatographic resolution of a ferrocene derivative was reported by Schlögl, who enantioseparated compound **47** on acetylated cellulose [15]. The partial

enantioseparations of ferrocenes **48** [167] and **49** [168] (Figure 11) were also obtained by the Schlögl's group on partially acetylated cellulose, with benzene as mobile phase, and on microcrystalline triacetylcellulose with ethanol, respectively. In particular, at that time, the enantioseparation of **49** provided poor results after only one run under medium-pressure chromatographic conditions. Thus, the partial enantioseparation required 16 cycles by using a recycling technique, although, after about 15 runs on a 30-cm column, the separation window got saturated due to the peak broadening, so that no further increase of enantiomeric purity could be achieved (Figure 12).

In 1985, Armstrong et al. reported the first successful enantioseparations of chiral ferrocenes by enantioselective HPLC [49]. In this study, 11 ferrocenes containing a chiral centre, as stereogenic unit, were enantioseparated on a β -cyclodextrin (CD)-bonded CSP by using methanol (MeOH)/water mixtures as mobile phases, obtaining α values ranging from 1.06 to 1.39. It is worth mentioning that in the early 1980s, several nonchromatographic studies by Breslow [169–171] and Takahashi [172] also reported that chiral recognition was possible between CDs and various enantiomeric ferrocene compounds. Later, other CD-based CSPs were used for the enantioseparation of ferrocenes featured by central chirality exclusively [51, 173–175]. Recently, sulfobutylether- β -CD was used as a chiral selector for the CE enantioseparation of chiral ferrocenes exclusively containing a chiral centre, as a chiral element [176].

In 1989, the first HPLC enantioseparations of planar chiral ferrocenes **50** and **51** (Figure 13A) were reported by Yamazaki et al. by using a β -CD-bonded column and a 47% MeOH/water mixture as mobile phase [177]. The enantioseparation of the ferrocene derivative **50** is reported in Figure 13B. Under the same elution conditions, the enantiomers of ferrocene **51** were eluted with retention times of 32.5 and 33.9 min, respectively. In 1991, the same group reported the first HPLC enantioseparations of planar chiral ferrocenes (compounds **50–55**) on a polysaccharide-based chiral column, the Chiralcel OD containing cellulose *tris*(3,5-dimethylphenylcarbamate) as chiral selector coated in silica gel, by using a *n*-hexane/2-propanol (2-PrOH) mixture as a mobile phase [178] (Table 1). Under these conditions, ferrocenes **54** and **55** were not eluted.

Given the versatility and the remarkable load capacity of the polysaccharide-based CSPs, in the second half of the 1990s, the first semipreparative HPLC enantioseparations of planar chiral ferrocenes were successfully performed by the Fu's group by using, in most cases, Chiralcel OD as a chiral column (Figure S7). In 1996, the enantioseparation of the planar chiral azaferrocene **56** with a Chiralcel OD column and *n*-hexane/2-PrOH 90:10 v/v as mobile phase [148] was performed, recovering each enantiomer with 98% *ee*. A year later, the same group

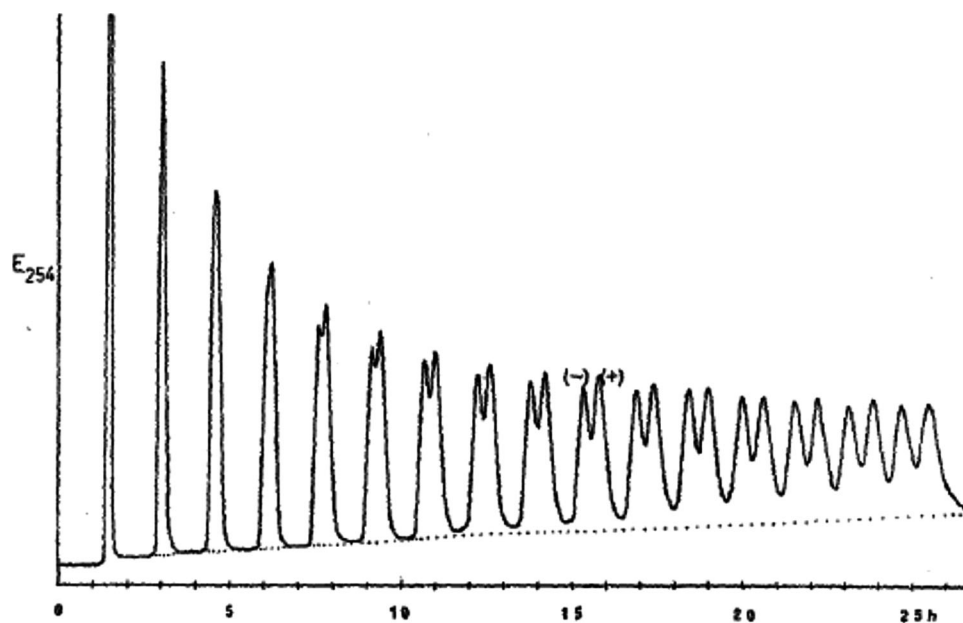


FIGURE 12 Chromatographic resolution of ferrocene **49** in 16 cycles under medium-pressure conditions. *Source:* Reprinted from Ref. [168] with permission

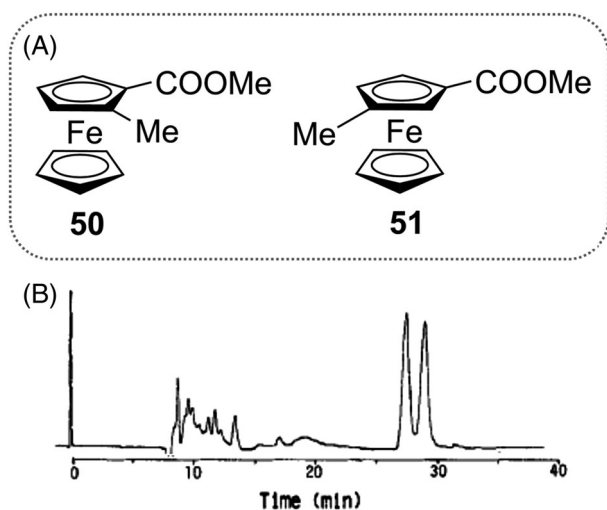


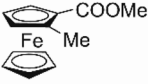
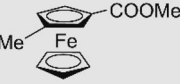
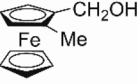
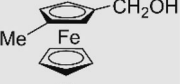
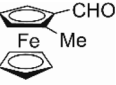
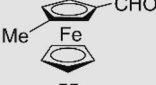
FIGURE 13 Structures of ferrocenes **50** and **51** (A), and enantioseparation of ferrocene **50** (B). Column, Cyclobond I; mobile phase, 47% MeOH/water; flow rate, 0.4 ml/min. *Source:* Adapted from Ref. [177] with permission

accessed pure enantiomers of azaferrocene **57** [179], and planar chiral 4-(dimethylamino)pyridine analogues **39** and **58** [28] again on Chiralcel OD, by using *n*-hexane/2-PrOH 90:10 v/v, *n*-hexane/2-PrOH/diethylamine (DEA) 50:50:0.2 v/v/v and *n*-hexane/2-PrOH/DEA 75:25:0.4 v/v/v, respectively, as mobile phases. In 1998, pure enantiomers of the C_2 -symmetric bisazaferrocene **59** were also recovered on Chiralcel OD (*n*-hexane/2-PrOH/DEA 95:5:0.1 v/v/v) with >99% *ee* [158]. Then, the semipreparative enantioseparation of phosphoferrocene **60** was also performed

on the Chiralcel OD (*n*-hexane/2-PrOH 90:10 v/v) [180]. It is worth mentioning that, later, the Fu's group also reported about the semipreparative enantioseparation of a C_2 -symmetric planar chiral bipyridine ligand with the brush-type column Whelk-O1 [181]. In the same period, Bolm et al. reported the first utilization of an amylose-based column, the Chiralpak AD, for the semipreparative enantioseparation of a planar chiral ferrocene, obtaining the pure enantiomers of the ferrocene-based hydroxyloxazoline **61** with >99.8% *ee* under normal phase conditions [26].

Despite the fact that the first enantioseparations of planar chiral ferrocenes were performed on a CD-based CSP [177], already at the dawn of planar chiral ferrocene enantioseparations polysaccharide-based CSPs emerged as privileged platforms to enantioseparate this class of organometallic compounds. As a result, in the last decades the enantioseparations of planar chiral ferrocenes have been performed by using polysaccharide-based CSPs almost exclusively, and just few enantioseparations with other types of chiral selectors were reported. In this regard, it is worth mentioning that the key structural elements of these polymeric selectors are the backbone (amylose or cellulose), and the pendant groups (phenylcarbamates or esters) which synergistically determine the distinctive resolving ability of the corresponding chiral columns (Table S2). The main interactions involving phenylcarbamate and ester (benzoate or cinnamate) pendant groups of these selectors are HBs, dipole-dipole and π - π interactions, along with XBs and chalcogen bonds [182]. However, these latter two types of interactions only

TABLE 1 First enantioseparations of planar chiral ferrocenes 50–55 on Chiralcel OD (*n*-hexane/2-PrOH mixture) [178]

Fc	k_1^a	k_2^a	α^b	R_s^c	EEO ^d
 50	0.63	0.88	1.39	2.94	R_p-S_p
 51	0.99	1.35	1.35	3.41	R_p-S_p
 52	2.27	2.58	1.14	1.81	S_p-R_p
 53	1.77	1.99	1.12	1.46	R_p-S_p
 54	Not eluted				
 55	Not eluted				

^aRetention factor.^bSelectivity factor.^cResolution.^dEnantiomer elution order.

participate in binding and recognition of analytes with specific structural requirements [183]. In particular, the methyl or/and chlorine substituents on the phenyl rings of the pendant groups modulate the electron charge density on the O=C–N–H moieties of the polymers, determining the strength of the carbonyl oxygens, as HB/XB acceptors, and of the amidic hydrogens, as HB donors. In Figure 14, for some representative polysaccharide-based selectors featuring chiral columns used in the enantioseparation of planar chiral ferrocenes over time (Table S2), the HB capability of the corresponding O=C–N–H moieties was compared by changing the distinctive substitution on the phenyl rings of the pendant groups. This comparison was performed in terms of the associated $V_{S,max}$ and V minima ($V_{S,min}$) calculated respectively for the amidic hydrogens and the carbonyl oxygens on isodensity surfaces [183].

In the next sections, enantioseparations of planar chiral ferrocenes performed on polysaccharide-based CSPs in the last decades will be described. For clarity, names and features of the chiral columns mentioned in the following sections are summarized in Table S2. The reported procedures will be categorized on the basis of the structural features of the analytes, determined in turn by the

distinctive substituents bound to the ferrocene moiety: (a) polar groups such as OH, C=O, COOH and COOR and others containing O and N atoms (Section 3.1), (b) substituents containing extended π -electronic clouds (Section 3.2) and (c) halogen atoms (Section 3.3). This choice is based on the fact that properties, functions and mechanisms of chiral chromatographic systems are based on concepts at the interface of analytical, physical and organic chemistry. Indeed, on the one hand, the enantioseparation process concerns the adsorption phenomenon underlying retention mechanism of analyte molecules which compete with solvent molecules onto the CSP surface [182]. On the other hand, chiral analytes, selectors and most mobile phase components are organic compounds. As a consequence, the structural properties (shape, geometry and electronic distribution) of the three pivotal components of the chromatographic system play a key role in the enantiodistinction processes. Considering these features may help analytical scientists to design enantioseparation procedures by evaluating steric and electronic properties of the molecular structures involved in the chromatographic system, going beyond trial-and-error approaches for methods development.

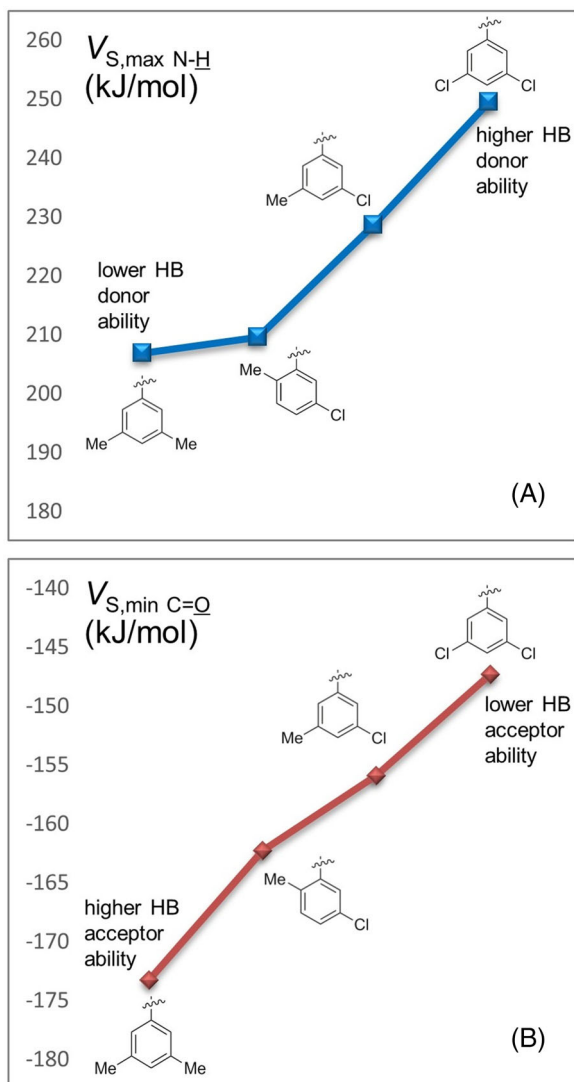


FIGURE 14 Comparison of $V_{S,max}$ (A) and $V_{S,min}$ (B) calculated for the amidic hydrogens and the carbonyl oxygens, respectively, on isodensity surfaces, for the 3,5-dimethyl-, 5-chloro-2-methyl-, 3-chloro-5-methyl- and 3,5-dichlorophenylcarbamates as pendant groups

3.1 | Planar chiral ferrocenes containing polar groups

Given that planar chiral ferrocenes with coordinative properties have attracted great interest for applications in several fields, most HPLC enantioseparations of planar chiral ferrocenes performed over time concern ferrocenes containing polar groups such as NH_2 , NHR , NRR_1 , C=O , COOH , COOR and OH . Following the pioneering studies of Schlögl [168] and Yamazaki [177], in 2002 the first analytical study on enantioseparation of ferrocene containing the carbonyl moiety as distinctive group was reported by Buchmeiser et al. [44]. In this study, the enantioseparation of planar chiral

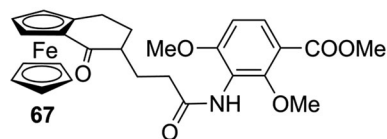


FIGURE 15 Structures of ferrocenocyclohexenone **67**

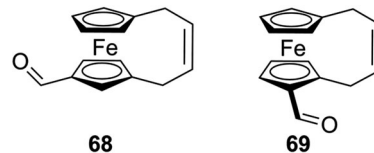


FIGURE 16 Structure of the bridge-substituted [3]ferrocenophanes **68** and **69**

ferroceno[2,3-a]inden-1-ones and derivatives was explored by using five homemade β -CD-based silica supports under polar organic conditions (ACN/MeOH/acetic acid/triethylamine [TEA] 99:1:0.1:0.1 v/v/v/v, $T = 0^\circ\text{C}$). The carbonyl moiety proved to be essential for achieving successful enantioseparation. Indeed, whereas ferroceno[2,3-a]inden-1-one (**62**) and derivatives could be enantioseparated with $1.62 \leq \alpha \leq 2.15$, ferroceno[2,3-a]indene (**63**) and alkoxyferroceno[2,3-a]indene (**64**) were not resolved. These first observations highlighted that the enantioseparation of nonpolar chiral planar ferrocenes may be rather challenging, this fact representing a still open issue. Again in 2002, in a paper reporting the synthesis of ferroquine enantiomers, Delhaes et al. mentioned the HPLC analytical enantioseparation of the 2-(*N,N*-dimethylaminomethyl)ferrocenecarboxaldehyde (**65**) and of the 2-(*N,N*-dimethylaminomethyl)ferrocenylmethyl acetate (**66**) by using the Chiralcel OD [118]. However, no other information was provided by the authors about these analyses. In 2011, Metzler-Nolte et al. reported the separation of the enantiomers (*R,R*_p) and (*S,S*_p) of the ferrocenocyclohexenone **67** (Figure 15) on Chiralpak IA under normal phase conditions (*n*-hexane/2-PrOH 60:40 v/v) [59]. Ferrocene **67**, featuring central and planar chirality, was prepared as intermediate for the synthesis of chiral ferrocene-containing platensimycin derivatives with potential antimicrobial activities. Recently, Buchowicz et al. reported the analytical enantioseparation of the bridge-substituted [3]ferrocenophanes **68** and **69** (Figure 16) used as synthetic intermediates for the synthesis of potential anticancer metallocenes [128]. For the purpose, Chiralcel OD-H and Chiralpak AD-H were used as chiral columns for the enantioseparation of **68** and **69**, respectively, the 1,3-disubstituted derivative being enantioseparated on the cellulose-based column (*n*-hexane/2-PrOH 95:5) better compared to the 1,2-disubstituted analogue on the Chiralpak AD-H

(*n*-hexane/EtOH 98:2). This couple of enantioseparations highlighted the fact that 1,2-disubstituted ferrocenes are often enantioseparated with lower α compared to the 1,3-disubstituted systems, likely due to the steric hindrance occurring between the two adjacent functional groups which may hinder selector–selectand interactions.

In several asymmetric synthesis studies, the determination of the enantiomeric purity of large series of structurally related planar chiral ferrocenes was performed. On the one hand, the evaluation of these chromatographic outcomes may allow for gaining information about structure–chromatographic behaviour relationships, accounting for the impact of analyte and selector structure, and of mobile phase polarity. Indeed, the chromatographic parameters, as well as the enantiomer elution order (EEO), are the macroscopic expressions of the enantioseparation process occurring at molecular level. In other words, they are signs of the noncovalent interaction between selector and selectand. On the other hand, in practice, only attempts to derive tentative guidelines for the enantioseparation of further planar chiral ferrocenes can be made given that a great variability of chromatographic conditions often occurs within these series of enantioseparations, and the systematic evaluation of the impact of a single factor may not be easy to derive.

In 2014, Cui et al. reported the first catalytic and enantioselective C–H direct acylation of ferrocene derivatives affording 17 2-acyl-1-dimethylaminomethylferrocenes (**36a–q**) with $56\% \leq ee \leq 98\%$ [40]. Determination of the enantiomeric purity was performed through enantioselective HPLC by using amylose-based Chiralcel IE-3 and cellulose-based Chiralcel IC-3 (Table S3), as chiral columns, both containing the 3,5-dichlorophenylcarbamate as a pendant group. By evaluating the chromatographic outcomes of ferrocenes **36a–q**, some remarks can be made:

1. Given the structure of analytes and selectors, it is likely that binding and recognition mechanisms are governed by HB occurring between the carbonyl oxygen of the analyte and the N–H of the selector pendant group, which is equal in both columns and with the highest HB donor ability (Figure 14).
2. The HB acceptor ability of the analytes is affected by the R substituent of the carbonyl moiety which modulates the electron charge density on the carbonyl oxygen and the steric hindrance of the neighbouring space. For instance, for the enantioseparations on the Chiralpak IC-3, both electronic and steric effects appeared to impact the enantioseparation. Indeed, under the same conditions, the enantioseparation of **36n** (R = Et) was lower than that of **36m** (R = Me), likely due to a negative steric impact of the alkyl chain. Then, the presence

of the chlorine, as an electron-withdrawing substituent, decreases the enantioseparation extent for **36o** and **36p** compared to the methylated compound **36q** (R = 3,4-dimethylphenyl). A similar effect also occurred on the Chiralpak IE-3. Indeed, considering compound **36c** (R = Ph) as reference for comparison, both ferrocenes **36a** and **36b**, containing strong electron-withdrawing groups such as F and CF₃, showed lower enantioseparation, the latter providing the lowest enantioseparation within the series **36**.

3. The EEO was always R_p – S_p on the amylose-based column, whereas a backbone-dependent EEO reversal (S_p – R_p) occurred on the Chiralpak IC-3. A single exception to this trend could be observed for the enantiomers of compound **36i** which were eluted on the Chiralpak IE-3 with the order S_p – R_p . In this regard, it could be noted that, among all compounds enantioseparated on the Chiralpak IE-3, only **36i** contains a furanyl group, as a distinctive substituent at the carbonyl moiety. This unit is more polar compared to the hydrophobic phenyl ring featuring all other derivatives and likely induces a mechanism change as revealed by the observed EEO reversal.

Later, You et al. reported the asymmetric synthesis of 22 planar chiral pyridine ferrocenopentadienone derivatives (**70a–v**) via Pd-catalysed intramolecular C–H arylation with high enantioselectivity (96%–99% *ee*), determining the enantiomeric purity of the prepared compounds by HPLC on polysaccharide-based Chiralcel OD-H, Chiralcel OJ-H, Chiralpak AD-H and Chiralpak AS-H, as chiral columns, with *n*-hexane/2-PrOH mixtures as mobile phases (Table S4) [29]. For these enantioseparations, some observations can be made as follows:

1. Twelve compounds (**70a–l**) were enantioseparated on Chiralcel OD-H with *n*-hexane/2-PrOH 90:10 v/v as mobile phase. Given compound **70a** as reference for comparison, it can be noted that structural variations of the groups R on the pyridine ring (**70i** and **70j**), or of R₁ on the other Cp ring (not containing the carbonyl group) (**70c–g**), or of both (**70k** and **70l**) do not produce EEO reversal, and in all these cases the enantiomers eluted as S_p – R_p . Otherwise, for compounds **70b** and **70h** showing structural variations at the two ‘external’ positions of the pyridine ring, an EEO reversal (R_p – S_p) occurred. Interestingly, despite the structural differences of the corresponding selectors, the same trend could be observed on the Chiralpak AD-H and on the Chiralpak AS-H for compounds **70o** and **70v**, respectively, showing R_p – S_p as EEO associated with structural variations of the external part of the pyridine rings. Otherwise, compounds which did not present this feature

such as **70n**, **70p**, **70q** and **70s–u** provided S_p – R_p as EEO.

- On the Chiralcel OD-H, the presence of fluorine as a substituent on the pyridine ring (**70l**: R = F, t_R = 7.7 min and 11.0 min) had a detrimental effect on retention and on the enantioseparation extent compared to the analogue containing an electron-donating group at the same position (**70k**: R = NMe₂, t_R = 10.9 and 21.2 min). On this column, the steric hindrance of the substituent R₁ impacted retention and selectivity. Thus, in compound **70f**, the presence of the bulky CHMe₂OH (t_R = 12.0 and 14.0 min) induced a decrease of retention compared to the analogue **70e** (t_R = 24.3 and 28.1 min). Otherwise, on Chiralpak AD-H, changing the methyl groups at the pentasubstituted Cp ring (**70p**: R₁ = Me, t_R = 5.5 and 5.8 min) to the ethyl groups (**70q**: R₁ = Et, t_R = 5.3 min and 6.4 min) decreased and increased the retention of the first and the second eluted enantiomers, respectively, and as a result, the enantioseparation extent increased.

In 2020, Guiry et al. reported the enantioseparation of the ferroceno[2,3-a]inden-1-one (**62**) under supercritical fluid chromatography (SFC) conditions (Chiralpak IB, scCO₂/2-PrOH 99:1 to 60:40 v/v over 7 min, EEO = S_p – R_p) for determining the enantiomeric purity (99% *ee*) of the compound used as intermediate for the synthesis of planar chiral ferrocifens [124].

Very recently, a first analytical study on the enantioseparation of planar chiral ferrocenes in SFC was reported by Lipka et al. [48]. In this study, the authors analysed several chiral metallocenes (M = Fe, Ru), among them five 1,2- and 1,3-disubstituted planar chiral ferrocenes, by using eleven polysaccharide-based CSPs (Lux Cellulose-2, Amylose-2 and Amylose-3, Chiralcel OD-H and OJ-H, Chiralpak IB, IC, AD-H, AS-H, IA and IG) with carbon dioxide containing 30% of MeOH or 2-PrOH as a co-solvent in the mobile phase. Among the planar chiral ferrocenes, one analyte contained two carbonyl groups, two derivatives featured amino moieties, and diphosphine and phosphamino derivatives were also included in the series. The elution of the analytes was optimized by adding 1% basic additive, such as DEA, TEA or *n*-butylamine to the mobile phase. In most cases, planar chiral ferrocenes involved in this study showed high retention and selectivity factors on the chlorinated cellulose-based CSPs which exhibited the highest rate of success compared to the non-chlorinated chiral supports. For instance, a resolution value equal to 14.1 was obtained for the enantioseparation of ferroquine **17** on the Chiralpak IC, based on the cellulose tris(3,5-dichlorophenylcarbamate) as a chiral selector, by using 30% 2-PrOH and 1% *n*-butylamine, whereas poor resolution was observed under

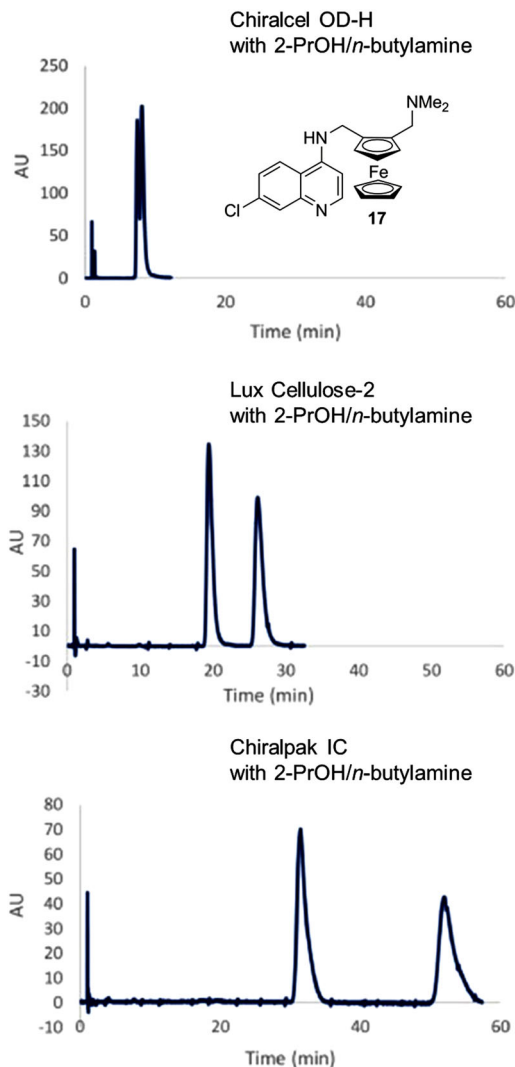


FIGURE 17 Chromatograms obtained for the enantiomers of compound **17** on Chiralcel OD-H, Lux Cellulose-2 and Chiralpak IC with 30% 2-PrOH and 1% of *n*-butylamine in carbon dioxide, at a flow-rate of 3 ml/min, column temperature of 40°C, 150-bar outlet pressure, λ = 260 nm. Source: Adapted from Ref. [48] with permission

the same conditions on the Chiralcel OD-H containing cellulose tris(3,5-dimethylphenylcarbamate) as a chiral selector (Figure 17). Moreover, the study evidenced interesting performances of the benzoate-type Chiralcel OJ-H towards the 1-[(1*R*)-1-(dicyclohexylphosphino)ethyl]-2-(diphenylphosphino)ferrocene **71** containing phenyl and cyclohexyl groups, as substituents of the P atom, which are able to exert π - π and hydrophobic interactions. This compound showed selectivity (α = 1.51) and resolution factors (R_s = 3.58) on this column higher compared to the more polar **17** (α = 1.32, R_s = 1.57). This study paves the way for interesting applications of SFC for the enantioseparation of planar chiral ferrocenes, in particular for preparative purposes.

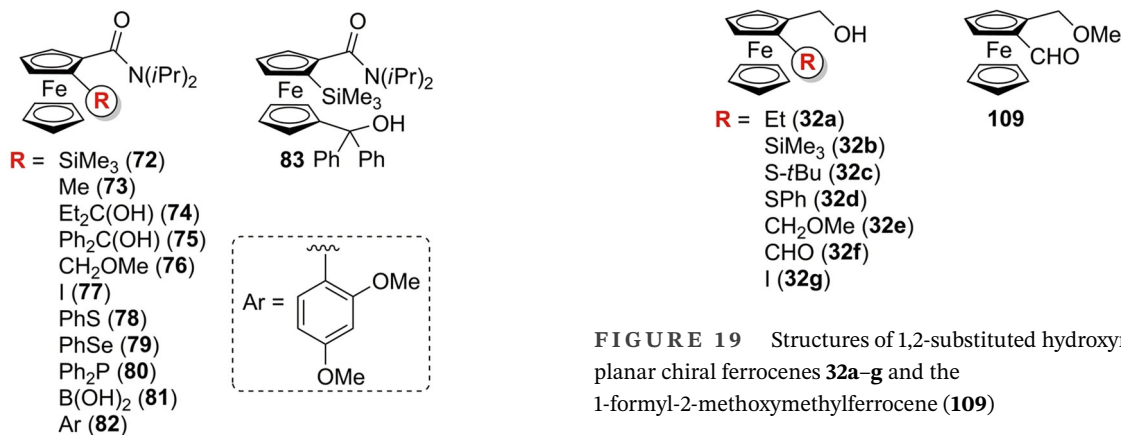


FIGURE 18 Structures of 1,2-substituted *N,N*-diisopropyl ferrocenecarboxamides **72–82** and of the 1,1',2-trisubstituted derivative **83**

Several enantioseparations for analytical purposes were reported involving planar chiral ferrocenes featured by the O=C–N– moiety. In 1996, Snieckus et al. reported the HPLC enantioseparation of 12 substituted *N,N*-diisopropyl ferrocenecarboxamides **72–83** (Figure 18) in order to establish the *ees* of the products prepared by asymmetric synthesis [37]. In this case, Chiralcel OD, OK and OJ were used as chiral columns. Almost all enantioseparations were performed by using *n*-hexane-based mixtures as mobile phases, with the exception of ferrocenes **73** and **81** which were enantioseparated by using aqueous–alcoholic mixtures (Table 2). Later, the same group reported the analytical enantioseparation of planar chiral *N*-cumyl-*N*-ethylferrocenecarboxamide **84**, *N*-ethylferrocenecarboxamides **85a–f**, methoxycarbonylferrocenes **86a–c**, ferrocenylpiperidinone **87**, ferrocenyldihydroazepinone **88** and ferrocenyltetrahydroazepinone **89** by using the Chiralcel OD, as chiral column, and *n*-hexane/2-PrOH mixtures as mobile phases (Table S5) [184]. In 2007, Whiting et al. reported the analytical enantioseparation of the analogue 2-bromo-(*N,N*-diisopropyl)ferrocenecarboxamide (**90**) on Chiralcel OD by using *n*-hexane/ether/DEA 80:20:0.5 v/v/v as mobile phase [151].

Very recently, large series of planar chiral alkylated ferrocene carboxamides **37a–h** and **91–97** (Table S6) [146], borylated ferrocenes **98a–y**, **99a–f** and **100–102**, and ferrocene carboxamide **103** (Table S7) [42], and ferrocene-fused pyridones **33a–u**, **104a–k** and **105** (Table S8) [142] were analytically enantioseparated on polysaccharide-based chiral columns under normal phase conditions. For compounds **98** and **99**, in most cases, Chiralpak IE and IC were used as chiral columns, in general, the latter providing lower retention times compared to the amylose-based column. Interestingly, compounds of the series **33**, **104** and

FIGURE 19 Structures of 1,2-substituted hydroxymethyl planar chiral ferrocenes **32a–g** and the 1-formyl-2-methoxymethylferrocene (**109**)

105 showed exceptional high optical rotation values up to $[\alpha]_D^{20} = +3665$.

In the last few years, planar chiral ferrocenes containing the ureido moiety were enantioseparated on polysaccharide-based CSPs. Tucker et al. determined the enantiomeric purity of the *N*-(4-nitrophenyl)-*N'*-[2-methyl-ferrocenemethyl]-urea **106** on Chiralpak AD (*n*-hexane/2-PrOH 90:10 v/v) [35]. Later, the same group reported the preparation of a series of hydroxyalkyl ferrocene-nucleosides (**107**) in order to evaluate their potential anticancer activity [131]. The enantiomers of these compounds were characterized by a combination of chiral analytical HPLC and single-crystal X-ray diffraction. In this frame, the enantiomeric purity of ferrocenes **107** was determined by using Lux Cellulose-1 as chiral column with 30% ACN in water as mobile phase. More recently, Erb et al. reported the enantioseparation (Chiralpak IC-3, *n*-hexane/2-PrOH 90:10 v/v) of the 4-(4-(3-(2-chloroferrocenyl)ureido)-3-fluorophenoxy)-*N*-methylpicolinamide **108** in the frame of a study on synthesis and biological evaluation of regorafenib analogues and their ferrocenic derivatives [132].

Over time, enantioseparations of planar chiral ferrocenes featured by hydroxyl groups were also described. Patti et al. reported the HPLC enantioseparation of 1,2-substituted hydroxymethyl ferrocenes **32a–d** [50] and **32e–g** [33], and of 1-formyl-2-methoxymethylferrocene (**109**) [33] on cellulose-based CSPs (Figure 19). The enantioseparations of ferrocenes **32a–d** were comparatively studied on Chiralcel OD and Chiralcel OJ as chiral columns under normal phase elution conditions [50]. All the alcohols **32a–d** were poorly retained and not sufficiently resolved on the Chiralcel OD, which appeared not suitable as chiral column for this type of analytes. On Chiralcel OJ, both **32a** and **32c** were eluted as single peaks, even with *n*-hexane/2-PrOH 99:1 v/v as mobile phase. Otherwise, a sufficient degree of enantioseparation was achieved for **32b** (*n*-hexane/2-PrOH 93:7 v/v; $k_2 = 1.04$, $\alpha = 1.23$, $R_s = 1.62$) and **32d** (*n*-hexane/2-PrOH 90:10 v/v:

TABLE 2 Enantioseparation conditions of planar chiral ferrocenes **72–83** (Figure 18) on cellulose-based chiral stationary phases (CSPs) [37]

Fc	Chiral column	Mobile phase	T (°C)	Flow rate (ml/min)
72	Chiralcel OD	1.5% <i>t</i> BuOMe in <i>n</i> -hexane	40	1.5
73	Chiralcel OJ	5% Water in ethanol (EtOH)	5	0.2
74	Chiralcel OD	10% (Et ₂ O/Et ₂ NH 0.5%) in <i>n</i> -hexane	rt ^a	1.0
75	Chiralcel OD	3% (Et ₂ O/Et ₂ NH 0.5%) in <i>n</i> -hexane	rt	1.5
76	Chiralcel OD	10% (Et ₂ O/Et ₂ NH 0.5%) in <i>n</i> -hexane	rt	0.9
77	Chiralcel OD	15% (Et ₂ O/Et ₂ NH 0.5%) in <i>n</i> -hexane	rt	1.0
78	Chiralcel OD	2% 2-PrOH in <i>n</i> -hexane	rt	0.5
79	Chiralcel OD	2% 2-PrOH in <i>n</i> -hexane	rt	0.5
80	Chiralcel OD	10% (Et ₂ O/Et ₂ NH 0.5%) in <i>n</i> -hexane	rt	1.5
81	Chiralcel OK	5% Water in MeOH	rt	1.0
82	Chiralcel OD	2% (Et ₂ O/Et ₂ NH 0.5%) in <i>n</i> -hexane	rt	1.5
83	Chiralcel OD	8% (Et ₂ O/Et ₂ NH 0.5%) in <i>n</i> -hexane	rt	1.5

^aRoom temperature.

TABLE 3 Enantioseparation of planar chiral ferrocenes **32e–g** and **109** on Lux Cellulose-2 (mobile phase, *n*-hexane/2-PrOH mixtures; flow rate, 0.5 ml/min) [33]

Fc	<i>n</i> -Hexane:2-PrOH (v/v)	<i>t</i> _{R1} (min) ^a	<i>t</i> _{R2} (min) ^a	EEO ^b
32e	85:15	25.01	38.53	S _p –R _p
32f	75:25	33.92	51.52	R _p –S _p
32g	90:10	20.62	24.81	S _p –R _p
109	75:25	19.58	23.91	R _p –S _p

^aRetention time.

^bEnantiomer elution order.

$k_2 = 13.14$, $\alpha = 2.88$, $R_s = 12.70$) on Chiralcel OJ, the latter ferrocene being resolved with higher α and R_s values. This result showed the pivotal role of the phenyl ring in the enantiodifferentiation process of this class of planar chiral ferrocenes on Chiralcel OJ. Very recently, in the course of a spectroscopic investigation on the chiroptical properties of ferrocenes **32e–g** and **109**, the same group performed the enantioseparation of these analytes by using the chlorinated Lux Cellulose-2, as chiral column, and *n*-hexane/2-PrOH mixtures, as mobile phases (Table 3 and Figure 20) [33]. It is worth noting that changing polar groups such as –CH₂OMe and –CHO, as substituents of the hydroxymethylferrocene scaffold (compounds **32e** and **32f**, respectively), to the hydrophobic iodine, featuring ferrocene **32g**, had a detrimental effect on the enantioseparation in terms of selectivity (Figure 20). Indeed, as mentioned earlier, the enantioseparation of ferrocenes containing nonpolar substituents exclusively is actually more challenging compared to that of polar ferrocenes.

The same group reported the enantioseparation of the planar chiral 1-acetyl-2-methoxymethylferrocene (**110**) on the Chiralcel OD by using *n*-hexane/2-PrOH

90:10 v/v as mobile phase [185]. In the same study, two ferrocenes containing both central and planar chirality were also enantioseparated under the same conditions, 1-acetoxyethyl-2-methoxymethylferrocene (**111**) ($t_R = 9.7$ min (1R_p,S) and 16.3 min (1S_p,R)) and the 1-hydroxyethyl-2-methoxymethylferrocene (**112**) ($t_R = 15.5$ min (1R_p,S) and 24.5 min (1S_p,R)). In both cases, the second diastereoisomer could not be resolved under the reported chromatographic conditions.

Very recently, ferrocene sulfonates have attracted interest as synthetic intermediates for the introduction of reactive groups such as SiMe₃ and I, and further functionalization [41]. In this frame, Erb et al. explored the possibility of obtaining enantioenriched derivatives **113** and **114** (Figure 21), determining their enantiomeric purity through HPLC analysis on Chiralpak IC-3 (*n*-hexane/2-PrOH = 98:2) and IA-3 (*n*-hexane/2-PrOH = 99:1), respectively. It is worth mentioning that the enantioseparation of the 2-(trimethylsilyl)ferrocenecarboxaldehyde (**115**) was also performed on a cellulose-based column (Chiralcel OD-H column, *n*-hexane/2-PrOH 99:1 v/v) [186].

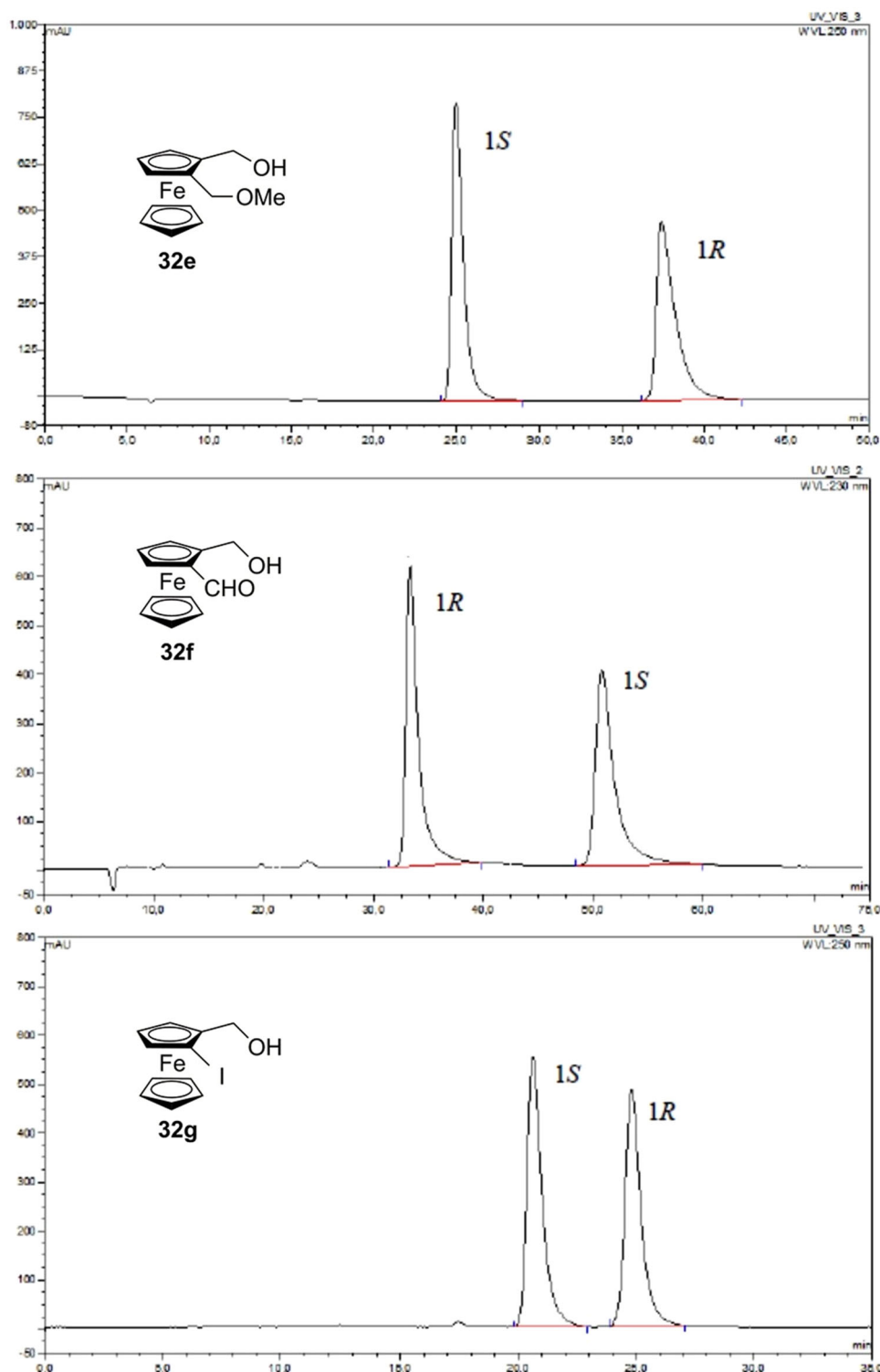


FIGURE 20 Chromatographic traces of the high-performance liquid chromatography (HPLC) enantioseparation of compounds **32e–g** on Lux Cellulose-2 (see Table 11 for elution conditions). *Source:* Adapted from Ref. [33] with permission

The enantioseparation of azaferrocenes was also reported by several groups. In 2001, Johannsen et al. reported the analytical enantioseparation of the sulfinyl azaferrocenes **56**, **116** and **117** (Figure S8) on the Chiralcel OD-H (*n*-hexane/2-PrOH 90:10 v/v) [161]. The

enantiomers S_S, S_P and R_S, S_P of the azaferrocene **116** were eluted at 12.1 and 10.9 min, respectively, whereas the enantiomers R_S, R_P and S_S, S_P of the other diastereoisomer remained unresolved under the adopted conditions. The enantiomers of compounds **117** ($t_R = 11.1$ min (R_P)) and

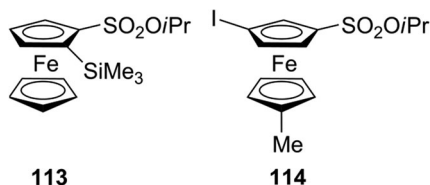


FIGURE 21 Structures of the isopropyl ferrocenesulfonate **113** and **114**

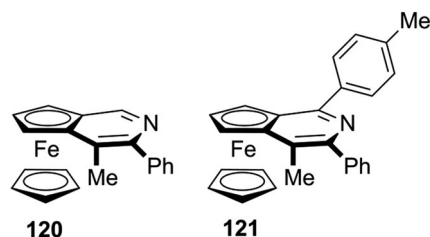


FIGURE 22 Structures of ferrocene-fused pyridines **120** and **121**

13.7 min (S_p) and **56** ($t_R = 11.4$ min (S_p) and 20.1 min (R_p)) were eluted with opposite elution order. In this case, it is interesting to note that the higher polarity of the distinctive substituent of **56** ($R = \text{CH}_2\text{OH}$) compared to **117** ($R = \text{I}$) affects the elution of the second eluted enantiomer, whereas the first eluted enantiomers of the two azaferrocenes are eluted almost equally. Later, Iwao et al. also reported the HPLC analytical enantioseparation of azaferrocenes by using Chiralpak AD with *n*-hexane/2-PrOH 19:1 v/v as mobile phase [159].

3.2 | Planar chiral ferrocenes containing aromatic groups and extended π -clouds

As mentioned previously, in the late 1990s Fu's group reported the semipreparative enantioseparation of the ferrocene-fused 4-(dimethylamino)pyridine analogue **39** [28]. This derivative was one of the first planar chiral ferrocenes, containing π -aromatic moieties, which were enantioseparated by enantioselective HPLC. Later, the same group reported the semipreparative enantioseparation of the 4-(methyl)- (**118**) [187] and the 4-(pyrrolidino)pyridine (**119**) [188] analogues on the Chiralcel OD by using *n*-hexane/ethyl acetate/DEA 97:3:0.4 v/v/v and *n*-hexane/ethanol/DEA 50:50:0.4 v/v/v as mobile phases, respectively. Very recently, Zheng et al. reported the enantioseparation of the two planar chiral ferrocene-fused pyridines **120** and **121** (Figure 22) by using Chiralcel OD-H (*n*-hexane/2-PrOH 95:5 v/v) and Chiralpak IG (*n*-hexane/2-PrOH 97:3 v/v), respectively, as chiral columns [142].

Starting from the 1980s [189], ferrocene helicenes, in which iron is included within the helical π -framework, have been recognized as valuable systems for optoelectronic applications [190]. Indeed, coordination of the extended π -electronic clouds to metal atoms impacts the electronic density distribution and, consequently, may change their properties. Given this context, in the last decade, enantioselective cycloisomerization reactions of 2-ethynyl-1-ferrocenylbenzene derivatives affording helical-shaped planar chiral ferrocenes have been investigated. In this context, the analytical enantioseparation of ferrocene-fused polycyclic benzenes has been reported by several groups.

In 2016, Shibata et al. reported the analytical enantioseparation of nine planar chiral ferrocene-fused polycyclic benzenes **122a–g**, **123** and **124** by using Chiralpak IA-3, IB-3 and IC-3 as chiral columns under normal phase conditions (Table 4) [143]. From the chromatographic data summarized in Table 4, it emerges that enantioseparation of halogenated planar chiral ferrocenes, which do not contain polar groups, may be rather challenging, requiring the use of mobile phases with low elution strength. Urbano et al. also reported the analytical enantioseparation of compound **30** and of other analogues of the series **122** by using Chiralpak IA, IB and IC, as immobilized chiral columns, and in almost all cases *n*-hexane/2-PrOH mixtures, as mobile phases [31, 191]. Interestingly, the enantioseparations of **122e** and two other fluorinated analogues were performed on the Chiralpak IA under SFC conditions (CO_2/MeOH 98:2) [191]. At the best of our knowledge, these represent the first examples of SFC enantioseparation of planar chiral ferrocenes reported in the literature.

In 2020, Lang et al. reported the successful discrimination of the enantiomers of planar chiral ferrocenes **29a,b**, **125** and **126a–c** (Figure 23) in voltammetry experiments on electrodes modified with electrodeposited inherently chiral oligomer films [34]. In this context, the chromatographic enantioseparations of these ferrocenes were carried out using the Chiralpak IG-3, as chiral column, with normal phase eluents. As shown in Figure 23, excellent enantiomer separation was achieved in all cases, and the process was scaled up to a semipreparative level, where both enantiomers could be collected in multi-milligram quantities.

Very recently, Cirilli et al. investigated the HPLC enantioseparation of the two series of planar chiral ferrocenes **29b–f** and **126a,d,e** on the Chiralpak AD-3, as chiral column (Figure 24) [47], considering compound **29a** as reference for comparison. Although the first series **29** carried different substituents on the styryl moiety, compounds **126** presented distinctive substituents on the thiophenyl moiety. The enantioseparations were carried out

using pure MeOH, EtOH, 1-PrOH and 2-PrOH as well as mixtures of *n*-hexane/2-PrOH as mobile phases. Interestingly, in this study, it was found that the enantioseparation extent was significantly influenced by elution modes and the steric hindrance of substituted aromatic rings. As shown in Figure 24, exceptional selectivity factors could be observed in certain conditions. For the unsubstituted **29a**, the enantioselectivity increased as the mobile phase changed from MeOH to 1-PrOH, ranging from 5.76 to 10.04. By using 2-PrOH, selectivity factor increased up to 55.51. For ferrocenes **126**, selectivity was less influenced by the nature of alcoholic eluent, the highest selectivity factor observed for **126d** with 2-PrOH as mobile phase ($\alpha = 14.07$). On this basis, the presence of substituents on the phenyl-thiophosphoryl fragment appeared to be detrimental for enantioseparation. For the series **29b–f**, the most remarkable difference in enantioselectivity was obtained with 2-PrOH, and the highest selectivity values were observed for compounds **29d** ($\alpha = 88.05$), **29e** ($\alpha = 87.33$) and **29f** ($\alpha = 84.68$). For all this type of exceptional enantioseparations, the EEO was S_p-R_p .

As reported earlier, moderate/high enantioselectivities can be obtained for planar chiral ferrocenes bearing polar substituents, whereas the enantioseparations of derivatives containing halogens, or exclusively alkyl groups, often proved to be rather challenging. In this regard, recently our groups explored the enantioseparation of 10 planar chiral 1,2- (**4**, **127a–d** and **128a,b**) and 1,3-disubstituted (**129a–c**) ferrocenes by using five polysaccharide-based CSPs (Lux Cellulose-1, i-Cellulose-5,

Amylose-1, i-Amylose-1 and i-Amylose-3) under multimodal elution conditions [45]. In this study, baseline enantioseparations were achieved for nine analytes with α ranging from 1.20 to 2.92 (Figure 25). Otherwise, 1-bromo-2-iodo-ferrocene (**128a**) could be only partially enantioseparated, confirming that the enantioseparation of small nonpolar planar chiral ferrocenes may be not easy due to the inherent structural inability of the enantiomers of this type of molecular systems to be enantiodifferentiated. In most cases, amylose-based CSPs provided better enantioseparation compared to cellulose-based ones. Moreover, due to the hydrophobic feature of the ferrocenes used in the study as analytes, aqueous methanol-containing MPs allowed for improving enantioseparation performances in several cases. Interestingly, for compound **129b**, the presence of π -extended systems in the analyte structure was shown to impact affinity of the most retained enantiomer towards amylose-based selectors, observing very high selectivity factor ($\alpha = 11.41$) with pure MeOH as mobile phase, with S_p-R_p as EEO (Figure 26A). In particular, it was observed that the addition of small amounts of MeOH to an *n*-hexane/2-PrOH mixture increased significantly the affinity of the second eluted enantiomers of both compounds **129b** and **129c**, producing large enantioseparation on amylose-based selectors. With the aim to disclose the origin of this phenomenon at molecular level, molecular dynamic (MD) simulations were performed by using the R_p -enantiomer of **129b** and a virtual model of the amylose tris(3,5-dimethylphenylcarbamate) (Figure 26B,C). This computational analysis confirmed (a)

TABLE 4 High-performance liquid chromatography (HPLC) enantioseparation of planar chiral ferrocene-fused polycyclic benzenes **122a–g**, **123** and **124** by using Chiralpak IA-3, IB-3 and IC-3 as chiral columns under normal phase conditions [143]

Fc	Column	Mobile phase, FR (ml/min) ^a	t_{R1} (min) ^b	t_{R2} (min) ^b
122a	IB-3	<i>n</i> -Hexane/2-PrOH 99:1, 0.5	14.6	17.1
122b	IC-3	<i>n</i> -Hexane/2-PrOH 99:1, 0.5	15.9	18.9
122c	IB-3	<i>n</i> -Hexane/2-PrOH 99:1, 0.5	18.3	21.0
122d	IA-3	<i>n</i> -Hexane/2-PrOH 99.5:0.5, 0.5	20.1	21.6
122e	IA-3	<i>n</i> -Hexane/2-PrOH 99.5:0.5, 0.5	20.1	21.9
122f	IA-3	<i>n</i> -Hexane/2-PrOH 99.5:0.5, 0.5	19.2	20.2
122g	IA-3	<i>n</i> -Hexane/2-PrOH 99.5:0.5, 0.5	19.2	25.2
123	IC-3	<i>n</i> -Hexane/2-PrOH 99:1, 1.0	14.3	17.8
124	IC-3	<i>n</i> -Hexane/2-PrOH 95:5, 1.0	7.9	14.2

^aFlow rate.

^bRetention time.

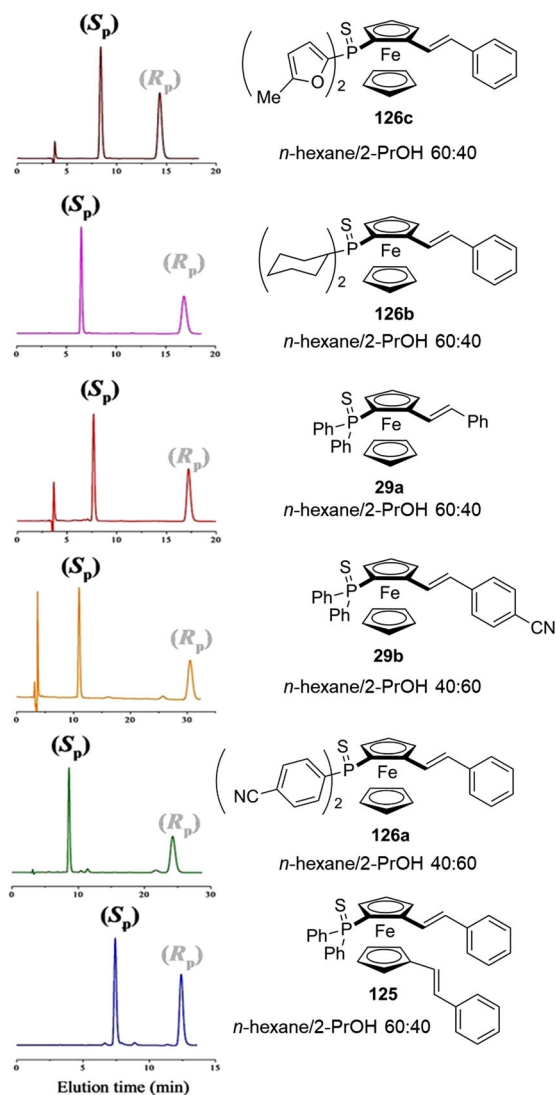


FIGURE 23 High-performance liquid chromatography (HPLC) enantioseparation of planar chiral ferrocenes **29a,b**, **125** and **126a–c** on Chiralpak IG. Source: Adapted from Ref. [34] with permission

the confinement of the analyte in a hydrophobic cavity deeply inside the selector groove and (b) the stabilization of the selector–selectand complex through an HB ($d = 2.347 \text{ \AA}$) between the ethynyl π -cloud and the amidic hydrogen of the selector as the molecular basis of the observed large enantioseparation.

In the last few years, several efforts have also been made to prepare enantiomerically enriched ferrocenes featured by π -electronic clouds. Indeed, the development of advanced computational methods has allowed to recognize that catalysts equipped with large aromatic groups may provide cumulative noncovalent interactions such as C–H $\cdots\pi$, N–H $\cdots\pi$ and $\pi\cdots\pi$ with a remarkable stabilization force on the catalytic transition states, often with the participation of dispersion forces [192]. In this frame,

in the last few years, the analytical enantioseparation of substituted 4-methyl-6-(methylsulfonyl)-6*H*-benzo[2,3]-azepino[4,5-*a*]ferrocenes **35a–g** (Table 5) [144], of 1-*N,N*-diisopropyl-2-substituted-ferroceneamides **130** (Figure S9) [193] and of 1-[(*2E*)-(4-substituted-benzylidene)-hydrazono]methyl]-2-substituted-ferrocenes **38** (Figure S9) [147] were reported. As shown in Table 5, for the enantioseparation of planar chiral ferrocenes containing extended π -electronic cloud regions, methylated polysaccharide-based selectors, in particular amylose-based ones, are preferred along with mobile phases featured by low eluting strength. However, under these conditions, phenomena of peak broadening and low resolution may be observed. Accordingly, for the analytical enantioseparation of 23 ferrocenes of the series **130**, in most cases chiral columns based on methylated polysaccharide selectors such as Chiralcel OD-3 and Chiralpak AD-H, and *n*-hexane/2-PrOH mixtures with 2-PrOH $\leq 2\%$ were used [193]. Analogously, in the case of 22 compounds of the series **38**, methylated Chiralpak AD-H and Chiralcel OD-H were used as chiral columns, exclusively [147].

3.3 | Planar chiral ferrocenes containing halogens as substituents

Halogenated ferrocenes are key intermediates for accessing polysubstituted ferrocenes [194]. More recently, iodinated ferrocenes were found to be involved in XB in solid state [106, 195], and even in solution with promising applications as organocatalysts in organic synthesis [87, 106].

In 2020, Kumar et al. described the analytical enantioseparation of the *N,N*-diisopropyl-2-iodoferroceneamide (**131**) on Chiralcel OD-3 with *n*-hexane/2-PrOH 98:2 v/v as mobile phase [193]. Later, Erb et al. reported the analytical enantioseparation of the series of iodinated planar chiral ferrocenes **132a–e** by using Chiralpak IA-3 and IC-3 as chiral columns under normal phase conditions (Table 6) [196]. It is worth noting that, given the hydrophobic character of iodine, the enantioseparation of some members of the series required the use of *n*-hexane-based mobile phases containing just 1% 2-PrOH.

Very recently, our groups explored systematically the enantioseparation of 11 dihalogenated planar chiral ferrocenes **1–5**, **128a**, **129a** and **133–136** by using 5 polysaccharide-based CSPs (Lux Cellulose-1, i-Cellulose-5, Amylose-1, i-Amylose-1 and i-Amylose-3) under multimodal elution conditions [46]. Baseline enantioseparations were achieved for nine analytes with α ranging from 1.15 to 1.66 (Figure 27). In this study, the

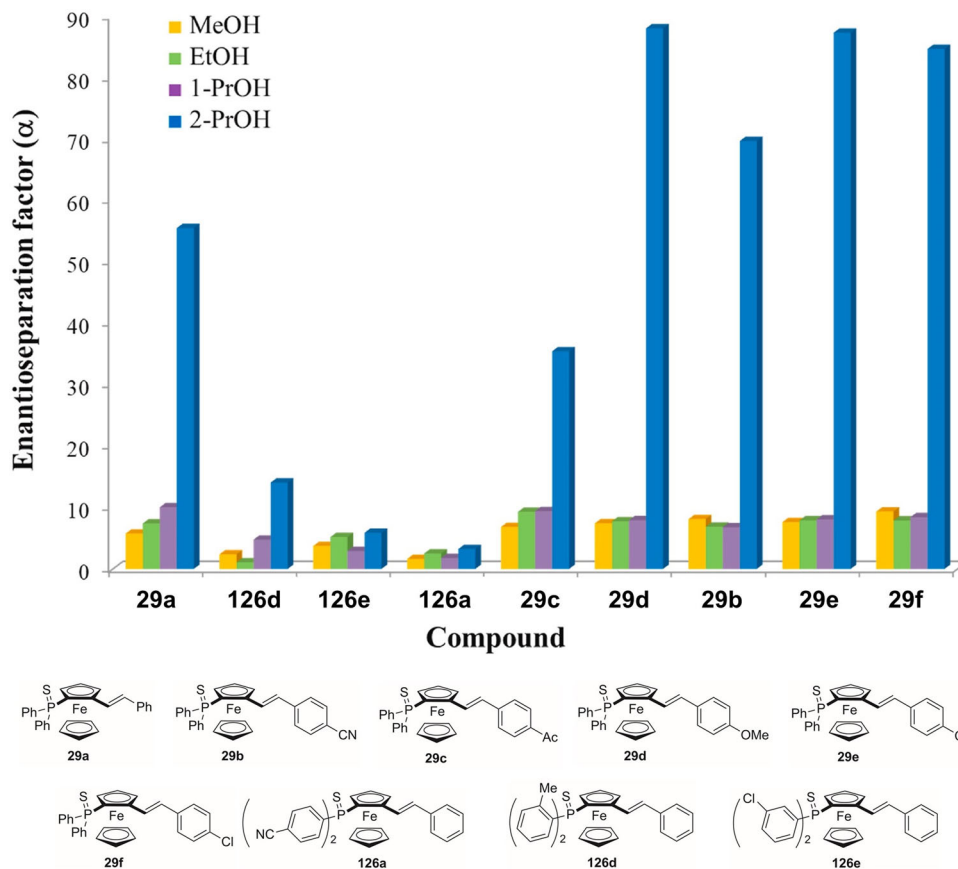


FIGURE 24 Effect of mobile phase on the enantioselectivity of ferrocenes **29a–f** and **126a,d,e** on Chiralpak AD-3. Source: Adapted from Ref. [47] with permission

TABLE 5 High-performance liquid chromatography (HPLC) enantioseparation of planar chiral substituted 4-methyl-6-(methylsulfonyl)-6H-benzo[2,3]-azepino[4,5-a]ferrocenes **35a–g** by using Chiralpak IA and IB-3 under normal phase conditions [193]

Fc	Column	Mobile phase, FR (ml/min) ^a	t _{RI} (min) ^b	t _{R2} (min) ^b
35a	IB-3	<i>n</i> -Hexane/2-PrOH 97:3, 1.0	20.0	21.6
35b	IA	<i>n</i> -Hexane/2-PrOH 97:3, 1.0	15.0	16.7
35c	IA	<i>n</i> -Hexane/2-PrOH 97:3, 1.0	12.0	12.8
35d	IA	<i>n</i> -Hexane/2-PrOH 97:3, 1.0	26.3	28.9
35e	IA	<i>n</i> -Hexane/2-PrOH 97:3, 1.0	17.2	19.2
35f	IA	<i>n</i> -Hexane/2-PrOH 99:1, 1.0	32.7	35.1
35g	IA	<i>n</i> -Hexane/2-PrOH 99:1, 1.0	32.8	35.7

^aFlow rate.

^bRetention time.

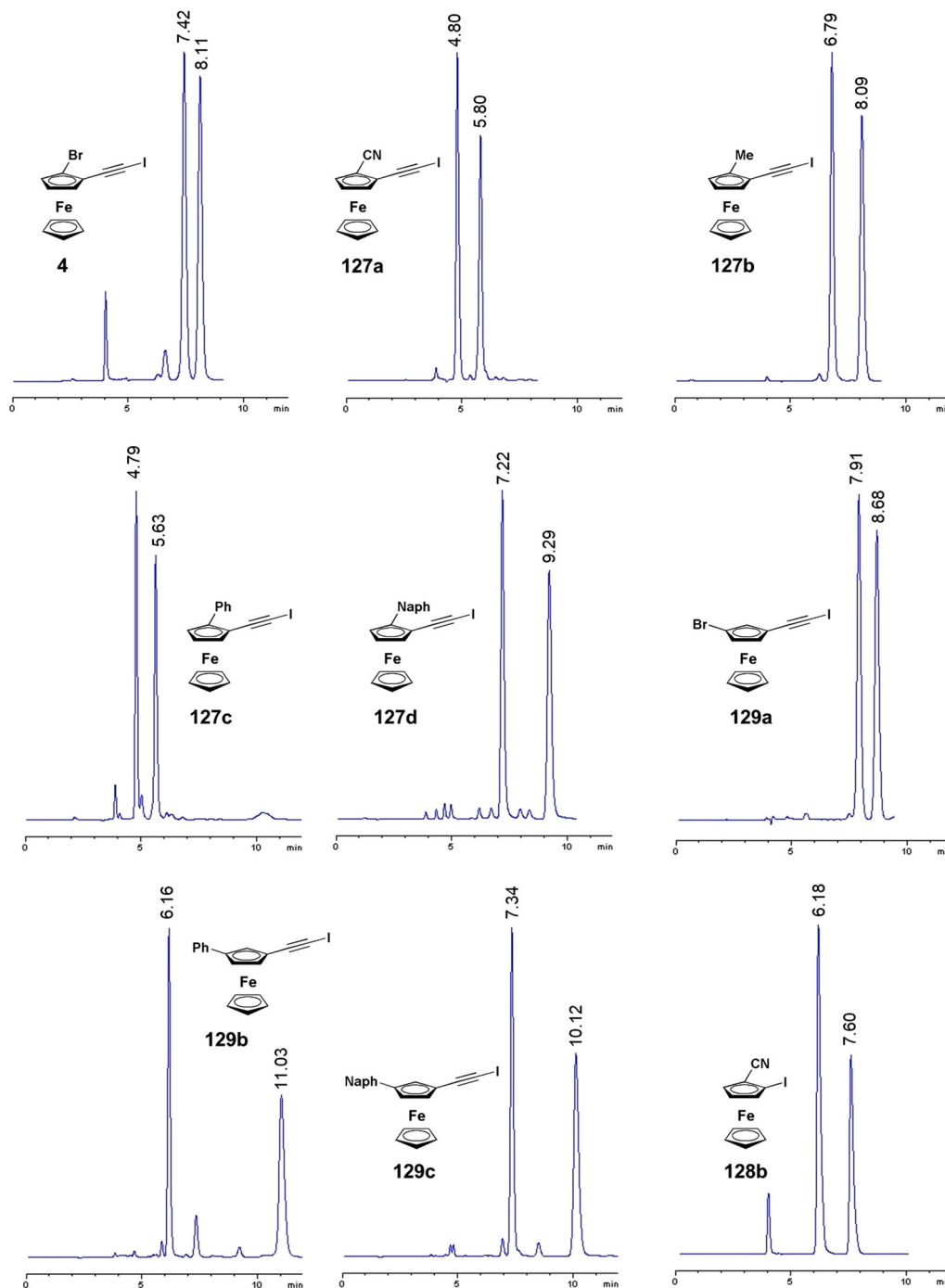


FIGURE 25 Baseline enantioseparation traces of compounds **4**, **127a–d**, **128b** and **129a–c**. Chromatographic conditions: **4**, Lux Amylose 1, MeOH/water 90:10; **127a**, Lux Amylose 1, MeOH/water 95:5; **127b**, Lux i-Amylose 3, MeOH/water 90:10; **127c**, Lux i-Amylose 3, MeOH 100%; **127d**, Lux i-Cellulose 5, *n*-hexane/2-PrOH 95:5; **129a**, Lux Amylose-1, MeOH 100%; **129b** and **129c**, Lux i-Amylose 3, *n*-hexane/2-PrOH 95:5; **128b**, Lux Cellulose-1, MeOH/water 95:5. Source: Adapted from Ref. [45] with permission

impact of CSP structure and mobile phase polarity on the enantioseparation was evaluated. In all cases, the best selectivity values were obtained by using Lux Amylose-1 and i-Amylose-3 as CSPs with methanol-containing mobile phases, with the exception of 1-bromo-2-iodo-ferrocene **128a** ($\alpha = 1.13$) and 1-fluoro-2-iodo-ferrocene **134** ($\alpha = 1.12$) which showed better enantioseparation

on Lux Cellulose-1. Moreover, the impact of halogen type and position on the enantioseparation was investigated by correlating theoretical and experimental data. For this purpose, thermodynamic quantities associated with the enantioseparations were derived from van't Hoff plots, and for 1-halo-2-(iodoethynyl)ferrocenes (1-halogen = F, Cl, Br) **2–4**, halogen-dependent

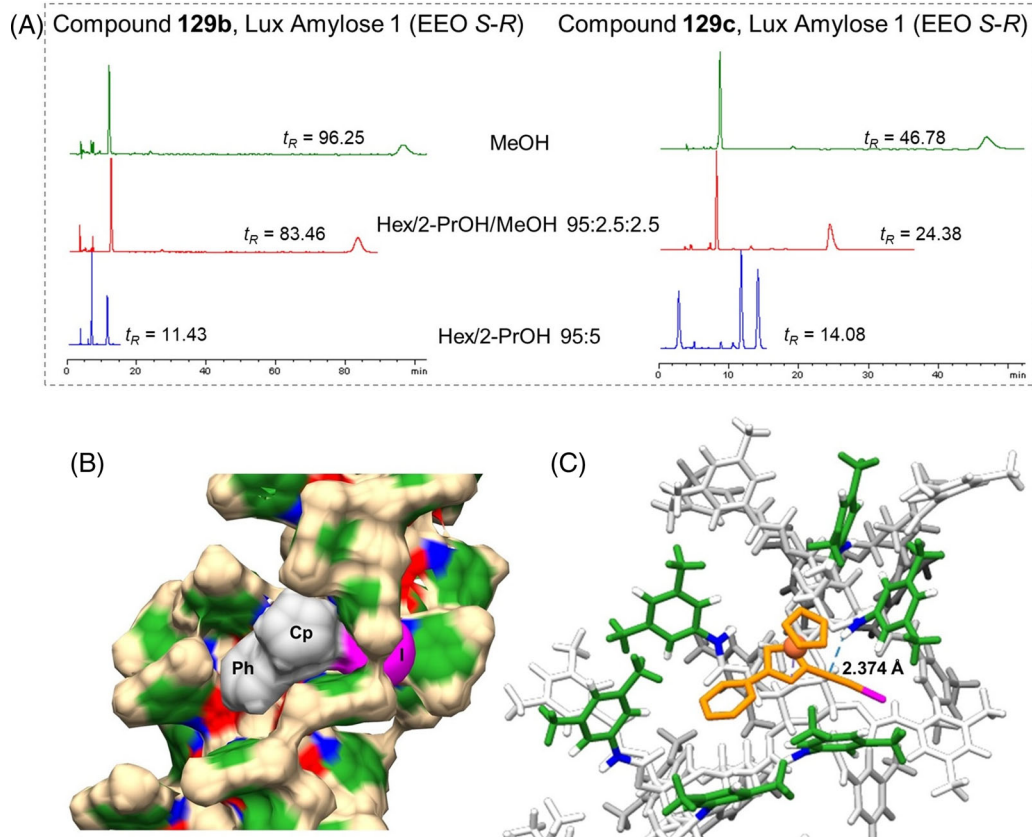


FIGURE 26 Comparison of the enantioseparation traces of compounds **129b** and **129c** on Lux Amylose 1, under multimodal elution conditions (A). Representative snapshot from the simulated MD trajectories (100 ns) of (R_p) -**129b** complex with amylose tris(3,5-dimethylphenylcarbamate) (solvent box, MeOH): (B) electron density surface (legend colors: green, aromatic ring; red, C=O; blue, N-H; gray, Ph + Cp + C≡C of (R_p) -**129b**; magenta, iodine) and (C) tube model of the (R_p) -**129b**/selector complex (legend colors: orange, Ph + Cp + Fe + C≡C of (R_p) -**129b**; magenta, iodine; green, aromatic rings featuring and delimiting the hydrophobic binding cavity of the selector). *Source:* Adapted from Ref. [45] with permission

TABLE 6 High-performance liquid chromatography (HPLC) enantioseparation of iodinated planar chiral ferrocene **132a–e** with Chiralpak IA-3 and IC-3 under normal phase conditions [196]

Fc	Column	Mobile phase, FR (ml/min) ^a	t_{R1} (min) ^b	t_{R2} (min) ^b	EEO ^c
132a	IC-3	<i>n</i> -Hexane/2-PrOH 99:1, 0.9	16.8	17.4	S_p - R_p
132b	IA-3	<i>n</i> -Hexane/2-PrOH 95:5, 1.0	7.0	7.3	S_p - R_p
132c	IC-3	<i>n</i> -Hexane/2-PrOH 90:10, 0.8	11.9	13.4	S_p - R_p
132d	IA-3	<i>n</i> -Hexane/2-PrOH 99:1, 0.5	11.0	11.7	R_p - S_p
132e	IA-3	<i>n</i> -Hexane/2-PrOH 99:1, 0.8	6.2	6.8	S_p - R_p

^aFlow rate.

^bRetention time.

^cEnantiomer elution order.

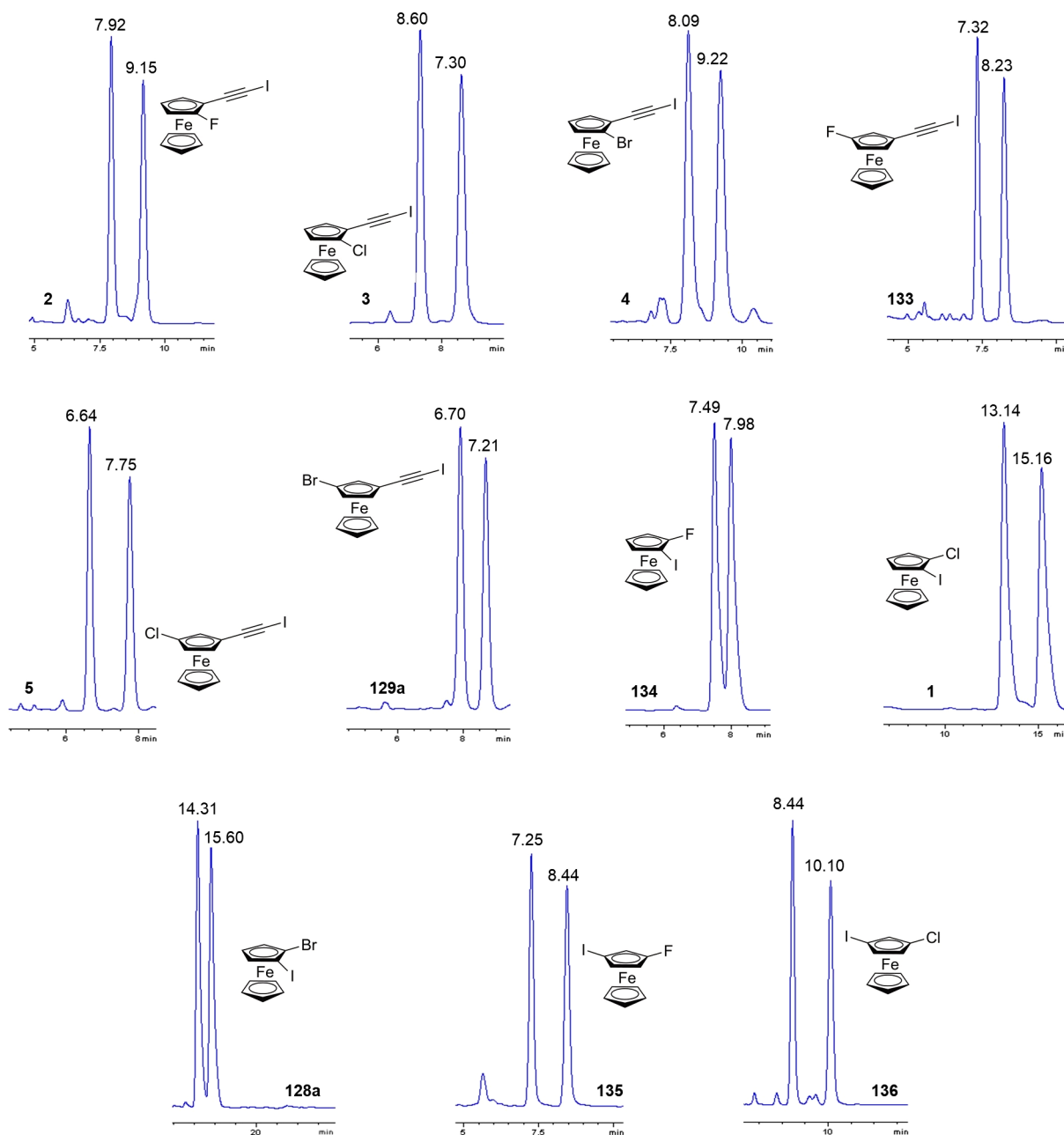


FIGURE 27 Baseline enantioseparation traces of compounds 1–5, 128a, 129a and 133–136. Chromatographic conditions ($T = 25^{\circ}\text{C}$ if not indicated otherwise): 2 and 3, Lux Amylose-1, MeOH/water 90:10 v/v; 4, Lux Amylose-1, MeOH/water 90:10 v/v ($T = 10^{\circ}\text{C}$); 133, Lux i-Amylose-1, MeOH/water 95:5 v/v; 5 and 129a, Lux Amylose-1, MeOH 100%; 134, Lux Cellulose-1, *n*-hexane/2-PrOH 95:5 v/v ($T = 5^{\circ}\text{C}$); 1 and 128a, Lux Cellulose-1, MeOH/water 90:10 v/v ($T = 5^{\circ}\text{C}$); 135 and 136, Lux Amylose-1, MeOH/water 95:5 v/v. Source: Adapted from Ref. [46] with permission

thermodynamic profiles were identified on the cellulose tris(3,5-dimethylphenylcarbamate)-based column (Figure 28). In particular, with the aim to unravel the functions of halogen substituents in mechanisms and noncovalent interactions underlying selector-selectand complex formation at molecular level, local electron charge density of specific molecular regions of the inter-

acting partners were evaluated in terms of calculated V and related source function contributions. On this basis, it was demonstrated that HB involving the NH group of the selector as the HB donor participates in the enantiodifferentiation mechanism for the fluorinated ferrocene 2, whereas an XB involving the carbonyl group of the selector occurred for the more polarizable 1-bromoferrocene 4.

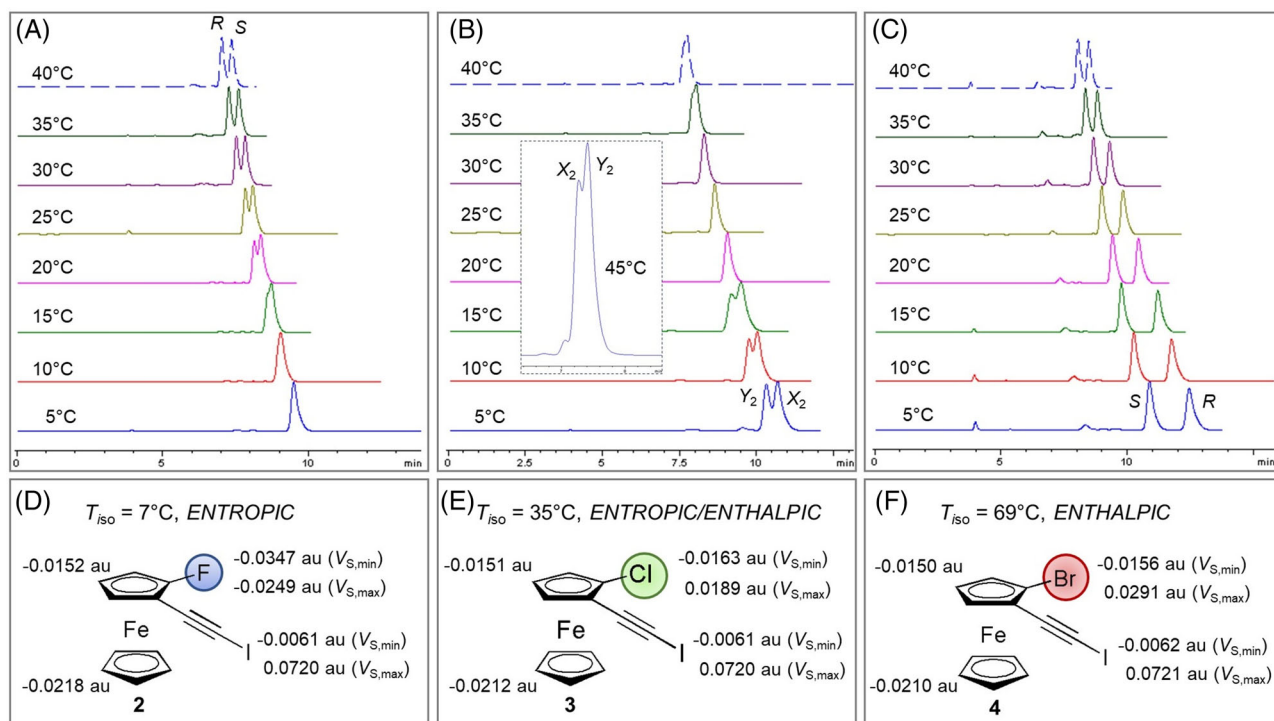


FIGURE 28 Enantioseparation of ferrocenes **2** (A), **3** (B) and **4** (C) at variable temperature on Lux Cellulose-1 with *n*-hexane/2-PrOH 95:5 v/v, and variation of the $V_{S,min}$ and $V_{S,max}$ values (D–F) as the 1-halogen substituent changes in the series of 1-halo-2-(iodoethynyl)ferrocenes **2–4**. Source: Adapted from Ref. [46] with permission

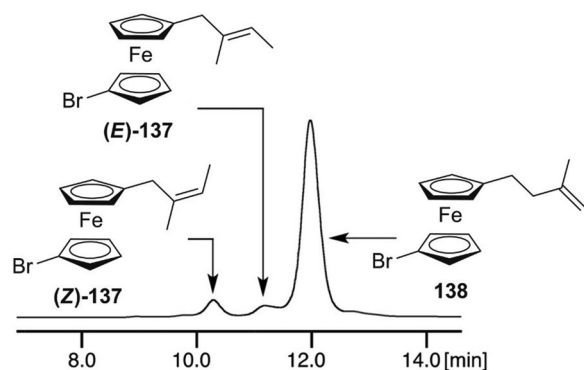


FIGURE 29 High-performance liquid chromatography (HPLC) traces for the mixture of (*E*)- and (*Z*)-**137** and **138** on Chiralpak IA using *n*-hexane as an eluent

It is worth mentioning that, recently, Ohnishi et al. used Chiralpak IA, IB and IC, for the separation of nonenantiomeric isomers of various ferrocenes. In particular, as shown in Figure 29, the (*E*)- and (*Z*)-isomers of 1-bromo-1'-(2-methyl-2-butenyl)ferrocene **137** and 1-bromo-1'-(3-methyl-3-butenyl)ferrocene **138** could be separated by using Chiralpak IA as column and pure *n*-hexane as mobile phase ($FR = 0.5$ ml/min) [197].

4 | CONCLUDING REMARKS

Chiral planar ferrocenes have been attracting a huge interest in several fields from asymmetric catalysis to medicinal chemistry, electrochemistry and chiroptical analysis. Despite that, the access to enantiopure or enantioenriched planar chiral ferrocenes on a wide scale is limited by the fact that a number of motifs still lack efficient asymmetric strategies. In this regard, enantioseparation science may definitely contribute to fill this gap. However, the overview of the studies developed over time suggests that these issues have been rather overlooked by analytical scientists. As a consequence, a huge number of enantioseparations of planar chiral ferrocenes have been carried out in the field of organic and organometallic asymmetric synthesis with the purpose to determine the enantiomeric excesses of chiral products, whereas few systematic analytical studies have been reported over time. Nowadays, electromigration techniques remain almost unexplored in this field, and only very recently the first CE enantioseparations of planar chiral ferrocenes were reported by the Lipka's group by using native and substituted CDs as chiral selectors [198].

Although the first enantioseparations of a planar chiral ferrocene were performed on CD-based chiral columns,

and some enantioseparations by using the Whelk-O1 column have also been reported, most analyses in this field have been performed by using polysaccharide-based CSPs. Due to the high load capacity of these CSPs, starting from the late 1990s, planar chiral ferrocene catalysts were available in their enantiopure form through preparative HPLC enantioseparation.

With the aim to obtain baseline enantioseparation ($R_s \geq 1.5$) of planar chiral ferrocenes, focused choices have to be done, in terms of chiral column and elution mode, which are strictly dependent on structure and properties of the substituents generating the chiral plane. In 1,2, n' - and 1,3, n' -trisubstituted planar chiral ferrocenes, the substituents at the n' position may impact retention and selectivity depending on their polarity and steric hindrance. On the basis of the results available so far, an attempt to profile some practical guidelines for approaching the enantioseparation of planar chiral ferrocenes with polysaccharide-based selectors can be made: (a) chlorinated polysaccharide-based ones were successfully used for the enantioseparation of polar ferrocenes containing carbonyl groups and carboxamide moieties; (b) otherwise, methylated polysaccharide-based CSPs showed better performances with nonpolar analytes. In these cases, methylated and chloromethylated amylose-based columns exhibit better performances compared to cellulose-based columns; (c) in general, ferrocenes containing nonpolar and hydrophobic groups may be challenging to enantioseparate under normal phase conditions. In this case, the elution strength of n -hexane-based mobile phases needs to be reduced by using percentages of 2-PrOH $\leq 5\%$. Alternatively, pure n -hexane or n -heptane may be used as mobile phase, although with these solvents peak broadening is not unusual, and the analytes may be poorly soluble in the mobile phase. In these cases, methanol-containing mixtures may provide better results in terms of selectivity factors compared to classical n -hexane/2-PrOH mixtures.

Recent studies have paved the way to new horizons, generating a renewed interest in the enantioseparation of planar chiral ferrocenes. On this basis, the new trends in this field are (a) *methods development and applications under SFC conditions*, which may open new possibilities for preparative enantioseparation of planar chiral ferrocenes. So far, just two groups performed SFC enantioseparations of planar chiral ferrocenes in the frame of organic synthesis studies [124, 191], and only recently the first analytical study under SFC conditions has been published [48]; (b) *methods based on the use of polar organic mode and aqueous-organic mixtures* which have been proven to be more efficient for the enantioseparation of nonpolar and hydrophobic ferrocene compared to the popular n -hexane/2-PrOH mixtures [45, 46]; (c) *mechanistic*

studies on high and exceptionally high enantioseparations provided by planar chiral ferrocenes featuring aromatic groups [45, 47]. This type of phenomena seems to be strictly dependent on polar solvents such as MeOH or 2-PrOH, proving that mobile phase, depending on its properties (polarity) may switch on or switch off some specific noncovalent interactions underlying binding and recognition; (d) *ferrocenes containing extended π -electronic clouds* may function as privileged test probes to explore π - π and dispersion forces in HPLC environment; (e) *halogenated ferrocenes containing electrophilically activated iodine substituents* were shown to participate in XBs under normal phase conditions; thus, halogenated ferrocenes may be used as test probes to explore properties and function of XBs in HPLC enantioseparation [46].

Despite the fact that integrating experimental and computational analysis represents a powerful tool to unravel the bases of enantioseparation mechanisms at the molecular level, modelling of ferrocene enantioseparation is still in its infancy. The first approaches to explore the enantioseparation of planar chiral ferrocenes by using computational techniques were developed only recently by our groups by using MD simulations, V analysis and related source function reconstruction [45, 46].

ACKNOWLEDGEMENTS

We thank the Consiglio Nazionale delle Ricerche (CNR), the University of Strasbourg and the Centre National de la Recherche Scientifique (CNRS) for financial support.

CONFLICT OF INTEREST

The authors have declared no conflict of interest.

DATA AVAILABILITY STATEMENT

The data that support the findings of this study are available from the corresponding author upon reasonable request.

ORCID

Paola Peluso  <https://orcid.org/0000-0003-3489-3428>

REFERENCES

1. Cahn RS, Ingold CK, Prelog V. The specification of asymmetric configuration in organic chemistry. *Experientia*. 1956;XII:81–94.
2. Verkade PE, Klesney SP, Cross LC, Dyson GM, Loening KL, Lozac'h N, et al. IUPAC tentative rules for the nomenclature of organic chemistry. Section E. Fundamental stereochemistry. *J Org Chem*. 1970;35:2849–67.
3. Hirschmann H, Hanson KR. Elements of stereoisomerism and prostereoisomerism. *J Org Chem*. 1971;36:3293–306.
4. Lemi re GL, Alderweireldt FC. Proposition for a new definition of the chiral plane and its consequences for the specification of planar chirality. *J Org Chem*. 1980;45:4175–9.

- Mislow K, Siegel J. Stereoisomerism and local chirality. *J Am Chem Soc.* 1984;106:3319–28.
- Moss GP. Basic terminology of stereochemistry (IUPAC Recommendations 1996). *Pure Appl Chem.* 1996;68:2193–222.
- López R, Palomo C. Planar chirality: a mine for catalysis and structure discovery. *Angew Chem Int Ed.* 2022;61:e202113504.
- Moss GP, Smith PAS, Tavernier D. Glossary of class names of organic compounds and reactivity intermediates based on structure (IUPAC Recommendations 1995). *Pure Appl Chem.* 1995;67:1307–75.
- Astruc D. Why is ferrocene so exceptional?. *Eur J Inorg Chem.* 2017;2017:6–29.
- Kealy TJ, Pauson PL. A new type of organo-iron compound. *Nature.* 1951;168:1039–40.
- Miller SA, Tebboth JA, Tremaine JF. 114. Dicyclopentadienyl-iron. *J Chem Soc.* 1952:632–5.
- Wilkinson G, Rosenblum M, Whiting MC, Woodward RB. The structure of iron bis-cyclopentadienyl. *J Am Chem Soc.* 1952;74:2125–6.
- Woodward RB, Rosenblum M, Whiting MC. A new aromatic system. *J Am Chem Soc.* 1952;74:3458–9.
- Werner H. At least 60 years of ferrocene: the discovery and rediscovery of the sandwich complexes. *Angew Chem Int Ed.* 2012;51:6052–8.
- Schlögl K. Configurational and conformational studies in the metallocene field. *Pure Appl Chem.* 1970;23:413–32.
- Schlögl K. Stereochemistry of metallocenes: 20 Years of progress and recent advances. *J Organomet Chem.* 1986;300:219–48.
- Schlögl K. Stereochemistry of metallocenes. *Top Stereochem.* 1967;1:39–91.
- Cahn RS, Ingold C, Prelog V. Specification of molecular chirality. *Angew Chem Int Ed.* 1966;5:385–415.
- Arae S, Ogasawara M. Catalytic asymmetric synthesis of planar-chiral transition-metal complexes. *Tetrahedron Lett.* 2015;56:1751–61.
- Moriuchi T. Helical chirality of ferrocene moieties in cyclic ferrocene-peptide conjugates. *Eur J Inorg Chem.* 2022;2022:e202100902.
- Arrayás RG, Adrio J, Carretero JC. Recent applications of chiral ferrocene ligands in asymmetric catalysis. *Angew Chem Int Ed.* 2006;45:7674–715.
- Cunningham L, Benson A, Guiry PJ. Recent developments in the synthesis and applications of chiral ferrocene ligands and organocatalysts in asymmetric catalysis. *Org Biomol Chem.* 2020;18:9329–70.
- Ferber B, Kagan HB. Metallocene sulfoxides as precursors of metallocenes with planar chirality. *Adv Synth Catal.* 2007;349:493–507.
- Mamane V. The diastereoselective ortho-lithiation of Kagan's ferrocenyl acetal. Generation and reactivity of chiral 2-substituted ferrocenecarboxaldehydes. *Tetrahedron: Asymmetry.* 2010;21:1019–29.
- Schaarschmidt D, Lang H. Selective syntheses of planar-chiral ferrocenes. *Organometallics.* 2013;32:5668–704.
- Bolm C, Muñoz-Fernández K, Seger A, Raabe G, Günther K. On the role of planar chirality in asymmetric catalysis: a study toward appropriate ferrocene ligands for diethylzinc additions. *J Org Chem.* 1998;63:7860–67.
- Muñiz K, Bolm C. Configurational control in stereochemically pure ligands and metal complexes for asymmetric catalysis. *Chem Eur J.* 2000;6:2309–16.
- Ruble JC, Latham HA, Fu GC. Effective kinetic resolution of secondary alcohols with a planar-chiral analogue of 4-(dimethylamino)pyridine. Use of the Fe(C5Ph5) group in asymmetric catalysis. *J Am Chem Soc.* 1997;119:1492–3.
- Gao D-W, Zheng C, Gu Q, You S-L. Pd-catalyzed highly enantioselective synthesis of planar chiral ferrocenylpyridine derivatives. *Organometallics.* 2015;34:4618–25.
- Singh A, Lumb I, Mehra V, Kumar V. Ferrocene-appended pharmacophores: an exciting approach for modulating the biological potential of organic scaffolds. *Dalton Trans.* 2019;48:2840–60.
- Urbano A, Del Hoyo AM, Martínez-Carrion A, Carreño MC. Asymmetric synthesis and chiroptical properties of enantiopure helical ferrocenes. *Org Lett.* 2019;21:4623–7.
- Ravutsov M, Dobrikov GM, Dangalov M, Nikolova R, Dimitrov V, Mazzeo G, et al. 1,2-Disubstituted planar chiral ferrocene derivatives from sulfonamide-directed ortho-lithiation: synthesis, absolute configuration, and chiroptical properties. *Organometallics.* 2021;40:578–90.
- Mazzeo G, Pedotti S, Longhi G, Patti A, Abbate S. Spectroscopic investigation on 1,2-substituted ferrocenes with only planar chirality: how chiroptical data are related to absolute configuration and to substituents. *Spectrochim Acta A Mol Biomol Spectrosc.* 2022;272:121010.
- Grecchi S, Arnaboldi S, Korb M, Cirilli R, Araneo S, Guglielmi V, et al. Widening the scope of “inherently chiral” electrodes: enantiodiscrimination of chiral electroactive probes with planar stereogenicity. *ChemElectroChem.* 2020;7:3429–38.
- Mulas A, Willener Y, Carr-Smith J, Joly KM, Male L, Moody CJ, et al. The effect of central and planar chirality on the electrochemical and chiral sensing properties of ferrocenyl urea H-bonding receptors. *Dalton Trans.* 2015;44:7268–75.
- Marquarding D, Klusacek H, Gokel G, Hoffmann P, Ugi I. Stereoselective syntheses. VI. Correlation of central and planar chirality in ferrocene derivatives. *J Am Chem Soc.* 1970;92:5389–93.
- Tsukazaki M, Tinkl M, Roglans A, Chapell BJ, Taylor NJ, Snieckus V. Direct and highly enantioselective synthesis of ferrocenes with planar chirality by (–)-sparteine-mediated lithiation. *J Am Chem Soc.* 1996;118:685–6.
- Gao DW, Gu Q, Zheng C, You SL. Synthesis of planar chiral ferrocenes via transition-metal-catalyzed direct C–H bond functionalization. *Acc Chem Res.* 2017;50:351–65.
- Šunjić V. Separation of enantiomers by chromatography as a vehicle for chiral catalysis. Abridged review. *Croat Chem Acta.* 2009;82:503–30.
- Pi C, Cui X, Liu X, Guo M, Zhang H, Wu Y. Synthesis of ferrocene derivatives with planar chirality via palladium-catalyzed enantioselective C–H bond activation. *Org Lett.* 2014;16:5164–7.
- Erb W, Wen M, Hurvois J-P, Mongin F, Halauko YS, Ivashkevich OA, et al. O-Isopropylferrocenesulfonate: synthesis of polysubstituted derivatives and electrochemical study. *Eur J Inorg Chem.* 2021;2021:3165–76.

42. Zou X, Li Y, Ke Z, Xu S. Chiral bidentate boryl ligand-enabled iridium-catalyzed enantioselective dual C–H borylation of ferrocenes: reaction development and mechanistic insights. *ACS Catal.* 2022;12:1830–40.
43. Ogasawara M, Wada S, Isshiki E, Kamimura T, Yanagisawa A, Takahashi T, et al. Enantioselective synthesis of planar-chiral ferrocene-fused 4-pyridones and their application in construction of pyridine-based organocatalyst library. *Org Lett.* 2015;17:2286–9.
44. Mayr B, Schottenberger H, Elsner O, Buchmeiser MR. Separation of planar chiral ferrocene derivatives on β -cyclodextrin-based polymer supports prepared via ring-opening metathesis graft-polymerization. *J Chromatogr A.* 2002;973:115–22.
45. Dessì A, Sechi B, Dallochio R, Chankvetadze B, Pérez-Baeza M, Cossu S, et al. Comparative enantioseparation of planar chiral ferrocenes on polysaccharide-based chiral stationary phases. *Chirality.* 2022;34:609–19.
46. Sechi B, Dessì A, Gatti C, Dallochio R, Chankvetadze B, Cossu S, et al. Unravelling functions of halogen substituents in the enantioseparation of halogenated planar chiral ferrocenes on polysaccharide-based chiral stationary phases: experimental and electrostatic potential analyses. *J Chromatogr A.* 2022;1673:463097.
47. Cantatore C, Korb M, Lang H, Cirilli R. ON/OFF receptor-like enantioseparation of planar chiral 1, 2-ferrocenes on an amylose-based chiral stationary phase: the role played by 2-propanol. *Anal Chim Acta.* 2022;1211:339880.
48. Bonin L, Morvan A, Coadou G, Furman C, Boulanger E, Ghinet A, et al. Supercritical fluid chromatography for separation of chiral planar metallocenes. *J Chromatogr A.* 2022;1674:463115.
49. Armstrong DW, DeMond W, Czech BP. Separation of metallocene enantiomers by liquid chromatography: chiral recognition via cyclodextrin bonded phases. *Anal Chem.* 1985;57:481–4.
50. Patti A, Pedotti S, Sanfilippo C. Comparative HPLC enantioseparation of ferrocenylalcohols on two cellulose-based chiral stationary phases. *Chirality.* 2007;19:344–51.
51. Li X, Zhou Z. Enantioseparation performance of novel benzimido- β -cyclodextrins derivatized by ionic liquids as chiral stationary phases. *Anal Chim Acta.* 2014;819:122–9.
52. Kovalevsky RA, Kucherenko AS, Korlyukov AA, Zlotin SG. Asymmetric conjugate addition of 3-hydroxychromen-4-ones to electron-deficient olefins catalyzed by recyclable C2-symmetric squaramide. *Adv Synth Catal.* 2022;364:426–39.
53. Snegur LV, Rodionov AN, Ostrovskaya LA, Ilyin MM, Simenel AA. Ferrocene-modified imidazoles: one-pot oxalyl chloride-assisted synthesis, HPLC enantiomeric resolution, and *in vivo* antitumor effects. *Appl Organomet Chem.* 2022;36:e6681.
54. Dai L-X, Tu T, You S-L, Deng W-P, Hou X-L. Asymmetric catalysis with chiral ferrocene ligands. *Acc Chem Res.* 2003;36:659–67.
55. Gibson VC, Long NJ, Oxford PJ, White AJP, Williams DJ. Ferrocene-substituted bis(imino)pyridine iron and cobalt complexes: toward redox-active catalysts for the polymerization of ethylene. *Organometallics.* 2006;25:1932–9.
56. Qiao L, Zhou X, Li X, Du W, Yu A, Zhang S, et al. Synthesis and performance of chiral ferrocene modified silica gel for mixed-mode chromatography. *Talanta.* 2017;163:94–101.
57. Hubbard PJ, Benzie JW, Bakhmutov VI, Blümel J. Ferrocene adsorbed on silica and activated carbon surfaces: a solid-state NMR study of molecular dynamics and surface interactions. *Organometallics.* 2020;39:1080–91.
58. Benecke J, Grape ES, Fuß A, Wöhlbrandt S, Engesser TA, Inge AK, et al. Polymorphous indium metal–organic frameworks based on a ferrocene linker: redox activity, porosity, and structural diversity. *Inorg Chem.* 2020;59:9969–78.
59. Patra M, Gasser G, Wenzel M, Merz K, Bandow JE, Metzler-Nolte N. Synthesis of optically active ferrocene-containing platensimycin derivatives with a C6–C7 substitution pattern. *Eur J Inorg Chem.* 2011;2011:3295–302.
60. Sansook S, Hassell-Hart S, Ocasio C, Spencer J. Ferrocenes in medicinal chemistry; a personal perspective. *J Organomet Chem.* 2020;905:121017.
61. Jaouen G, Vessières A, Top S. Ferrocifen type anti cancer drugs. *Chem Soc Rev.* 2015;44:8802–17.
62. Larik FA, Saeed A, Fattah TA, Muqadar U, Channar PA. Recent advances in the synthesis, biological activities and various applications of ferrocene derivatives. *Appl Organomet Chem.* 2017;31:e3664.
63. Patra M, Gasser G. The medicinal chemistry of ferrocene and its derivatives. *Nat Rev Chem.* 2017;1:0066.
64. Fabbrizzi L. The ferrocenium/ferrocene couple: a versatile redox switch. *ChemTexts.* 2020;6:22.
65. Kovač V, Kodrin I, Radošević K, Molčanov K, Adhikari B, Kraatz H-B, et al. Oxalamide-bridged ferrocenes: conformational and gelation properties and *in vitro* antitumor activity. *Organometallics.* 2022;41:920–36.
66. Patti A, Pedotti S, Mazzeo G, Longhi G, Abbate S, Paoloni L, et al. Ferrocenes with simple chiral substituents: an in-depth theoretical and experimental VCD and ECD study. *Phys Chem Chem Phys.* 2019;21:9419–32.
67. Baker AW, Bublitz DE. Enthalpies of intramolecular interactions in ferrocenyl alcohols. *Spectrochim Acta.* 1966;22:1787–99.
68. Glidewell C, Klar RB, Lightfoot P, Zakaria CM, Ferguson G. Hydrogen bonding in [alpha]-ferrocenyl alcohols: structures of 1-ferrocenylethanol, 1-ferrocenyl-2-phenylethanol, 1-ferrocenyl-1-phenylpropan-1-ol, 1-ferrocenyl-1-phenyl-2-methylpropan-1-ol, 1-ferrocenyl-1-phenyl-2,2-dimethylpropan-1-ol, 1-ferrocenyl-1,2-diphenylethanol and diferrocenyl(phenyl)methanol. *Acta Cryst.* 1996;B52:110–21.
69. Bailey RT, Lippincott ER. The vibrational spectrum of dimethylferrocene. *Spectrochim Acta.* 1965;21:389–98.
70. Coriani S, Haaland A, Helgaker T, Jørgensen P. The equilibrium structure of ferrocene. *ChemPhysChem.* 2006;7:245–9.
71. Haaland A, Nilsson JE. The determination of barriers to internal rotation by means of electron diffraction. Ferrocene and ruthenocene. *Acta Chem Scand.* 1968;22:2653–70.
72. Duggan DM, Hendrickson DN. Electronic structure of various ferrocenium systems as inferred from Raman, infrared, low-temperature electronic absorption, and electron paramagnetic resonance measurements. *Inorg Chem.* 1975;14:955–69.
73. Peluso P, Dessì A, Dallochio R, Mamane V, Cossu S. Recent studies of docking and molecular dynamics simulation for liquid-phase enantioseparations. *Electrophoresis.* 2019;40:1881–96.
74. Peluso P, Chankvetadze B. Native and substituted cyclodextrins as chiral selectors for capillary electrophoresis enan-

- tioseparations: structures, features, application, and molecular modeling. *Electrophoresis*. 2021;42:1676–708.
75. Sardella R, Camaioni E, Macchiarulo A, Gioiello A, Marinozzi M, Carotti A. Computational studies in enantioselective liquid chromatography: forty years of evolution in docking- and molecular dynamics-based simulations. *TrAC Trends Anal Chem*. 2020;122:115703.
 76. Lüthi HP, Ammeter JH, Almlöf J, Faegri K. How well does the Hartree–Fock model predict equilibrium geometries of transition metal complexes? Large-scale LCAO–SCF studies on ferrocene and decamethylferrocene. *J Chem Phys*. 1982;77:2002–9.
 77. Bohn RK, Haaland A. On the molecular structure of ferrocene, $\text{Fe}(\text{C}_5\text{H}_5)_2$. *J Organomet Chem*. 1966;5:470–6.
 78. Koch H, Jørgensen P, Helgaker T. The molecular structure of ferrocene. *J Chem Phys*. 1996;104:9528–30.
 79. Mohammadi N, Ganesan A, Chantler CT, Wang F. Differentiation of ferrocene D5d and D5h conformers using IR spectroscopy. *J Organomet Chem*. 2012;713:51–9.
 80. Wang F, Islam S, Vasilyev V. Ferrocene orientation determined intramolecular interactions using energy decomposition analysis. *Materials*. 2015;8:7723–37.
 81. Latouche C, Palazzetti F, Skouteris D, Barone V. High-accuracy vibrational computations for transition-metal complexes including anharmonic corrections: ferrocene, ruthenocene, and osmocene as test cases. *J Chem Theory Comput*. 2014;10:4565–73.
 82. Yáñez-S M, Moya SA, Zúñiga C, Cárdenas-Jirón G. Theoretical assessment of TD–DFT applied to a ferrocene-based complex. *Comput Theor Chem*. 2017;1118:65–74.
 83. Wen M, Erb W, Mongin F, Halauko YS, Ivashkevich OA, Matulis VE, et al. Functionalization of N,N-dialkylferrocenesulfonamides toward substituted derivatives. *Organometallics*. 2021;40:1129–47.
 84. Bogdanović GA, Novaković SB. Rigid ferrocene–ferrocene dimer as a common building block in the crystal structures of ferrocene derivatives. *CrystEngComm*. 2011;13:6930–2.
 85. Vargas-Caamal A, Pan S, Ortiz-Chi F, Cabellos JL, Boto RA, Contreras-Garcia J, et al. How strong are the metallocene–metallocene interactions? Cases of ferrocene, ruthenocene, and osmocene. *Phys Chem Chem Phys*. 2016;18:550–6.
 86. Grimme S. Semiempirical GGA-type density functional constructed with a long-range dispersion correction. *J Comput Chem*. 2006;27:1787–99.
 87. Mamane V, Peluso P, Aubert E, Weiss R, Wenger E, Cossu S, et al. Disubstituted ferrocenyl iodo- and chalcogenoalkynes as chiral halogen and chalcogen bond donors. *Organometallics*. 2020;39:3936–50.
 88. Togni A, Hayashi T. *Ferrocenes: homogeneous catalysis, organic synthesis, material science*. Weinheim: Wiley-VCH; 1995.
 89. Mamane V. Metal-catalyzed cross-coupling reactions for ferrocene functionalization: recent applications in synthesis, material science and asymmetric catalysis. *Mini-Rev Org Chem*. 2008;5:303–12.
 90. Sutcliffe OB, Bryce MR. Planar chiral 2-ferrocenyloxazolines and 1, 1'-bis (oxazoliny) ferrocenes—syntheses and applications in asymmetric catalysis. *Tetrahedron: Asymmetry*. 2003;14:2297–325.
 91. Togni A, Breutel C, Schnyder A, Spindler F, Landert H, Tijani A. A novel easily accessible chiral ferrocenyldiphosphine for highly enantioselective hydrogenation, allylic alkylation, and hydroboration reactions. *J Am Chem Soc*. 1994;116:4062–6.
 92. Spindler F, Malan C, Lotz M, Kesselgruber M, Pittelkow U, Rivas-Nass A, et al. Modular chiral ligands: the profiling of the Mandyphos and Taniaphos ligand families. *Tetrahedron: Asymmetry*. 2004;15:2299–306.
 93. Sturm T, Weissensteiner W, Spindler F. A novel class of ferrocenyl-aryl-based diphosphine ligands for Rh- and Ru-catalysed enantioselective hydrogenation. *Adv Synth Catal*. 2003;345:160–4.
 94. Hansen KB, Hsiao Y, Xu F, Rivera N, Clausen A, Kubryk M, et al. Highly efficient asymmetric synthesis of sitagliptin. *J Am Chem Soc*. 2009;131:8798–804.
 95. Blaser H-U, Brieden W, Pugin B, Spindler F, Studer M, Togni A. Solvias Josiphos ligands: from discovery to technical applications. *Top Catal*. 2002;19:3–16.
 96. Toma Š, Csizmadiová J, Mečiarová M, Šebesta R. Ferrocene phosphane-heteroatom/carbon bidentate ligands in asymmetric catalysis. *Dalton Trans*. 2014;43:16557–79.
 97. Zhu JC, Cui DX, Li YD, Jiang R, Chen WP, Wang PA. Ferrocene as a privileged framework for chiral organocatalysts. *ChemCatChem*. 2018;10:907–19.
 98. Bernardo O, González-Pelayo S, López LA. Synthesis and applications of ferrocene-fused nitrogen heterocycles. *Eur J Inorg Chem*. 2022;2022:e202100911.
 99. Yoshida K, Liu Q, Yasue R, Wada S, Kimura R, Konishi T, et al. Versatile and enantioselective preparation of planar-chiral metallocene-fused 4-dialkylaminopyridines and their application in asymmetric organocatalysis. *ACS Catal*. 2020;10:292–301.
 100. Fu GC. Asymmetric catalysis with “planar-chiral” derivatives of 4-(dimethylamino)pyridine. *Acc Chem Res*. 2004;37:542–7.
 101. Wang J, Zhu ZH, Chen MW, Chen QA, Zhou YG. Catalytic biomimetic asymmetric reduction of alkenes and imines enabled by chiral and regenerable NAD(P)H models. *Angew Chem Int Ed*. 2019;58:1813–7.
 102. Wang J, Zhao ZB, Zhao Y, Luo G, Zhu ZH, Luo Y, et al. Chiral and regenerable NAD(P)H models enabled biomimetic asymmetric reduction: design, synthesis, scope, and mechanistic studies. *J Org Chem*. 2020;85:2355–68.
 103. Janssen-Müller D, Schleppehorst C, Glorius F. Privileged chiral N-heterocyclic carbene ligands for asymmetric transition-metal catalysis. *Chem Soc Rev*. 2017;46:4845–54.
 104. Yoshida K, Yasue R. Planar-chiral ferrocene-based N-heterocyclic carbene ligands. *Chem Eur J*. 2018;24:18575–86.
 105. Fitzpatrick KP, Schwamb CB, Check CT, Jang K-P, Barsoum DN, Scheidt KA. Development of ferrocene-based planar chiral imidazopyridinium salts for catalysis. *Organometallics*. 2020;39:2705–12.
 106. Aubert E, Doudouh A, Wenger E, Sechi B, Peluso P, Pale P, et al. Chiral ferrocenyl-iodotriazolones and -iodotriazoliums as halogen bond donors. Synthesis, solid state analysis and catalytic properties. *Eur J Inorg Chem*. 2022;2022:e202100927.
 107. Sakai S, Kanemoto K, Fukuzawa S-I. Synthesis and evaluation of novel planar-chiral monophosphine ligands bearing ferrocene-triazole backbones. *Eur J Inorg Chem*. 2022;2022:e202100967.

108. Arthurs RA, Hughes DL, Richards CJ. Application of a ferrocene-based palladacycle precatalyst to enantioselective aryl-aryl Kumada coupling. *Eur J Inorg Chem.* 2022;2022:e202101077.
109. Caniparoli U, Escofet I, Echavarren AM. Planar chiral 1,3-disubstituted ferrocenyl phosphine gold(I) catalysts. *ACS Catal.* 2022;12:3317–22.
110. Meaney K, Goddard R, Bronger RPJ, Guiry PJ. The preparation of ferrocene-containing phosphinamine ligands possessing central and planar chirality and their application in palladium-catalysed allylic substitution. *Tetrahedron.* 2021;90:132088.
111. Zheng Y, Qin T, Zi W. Enantioselective inverse electron demand (3 + 2) cycloaddition of palladium-oxyallyl enabled by a hydrogen-bond-donating ligand. *J Am Chem Soc.* 2021;143:1038–45.
112. Yi X, Chen Y, Huang A, Song D, He J, Ling F, et al. Design of chiral ferrocenylphosphine-spiro phosphonamidite ligands for ruthenium-catalyzed highly enantioselective coupling of 1,2-diols with amines. *Org Chem Front.* 2021;8:6830–6.
113. O'Connor TJ, Mai BK, Nafie J, Liu P, Toste FD. Generation of axially chiral fluoroallenes through a copper catalyzed enantioselective β -fluoride elimination. *J Am Chem Soc.* 2021;143:13759–68.
114. Zeng L, Yang H, Zhao M, Wen J, Tucker JHR, Zhang X. *CI*-symmetric PNP ligands for manganese-catalyzed enantioselective hydrogenation of ketones: reaction scope and enantioinduction model. *ACS Catal.* 2020;10:13794–9.
115. Hartinger CG, Dyson PJ. Bioorganometallic chemistry—from teaching paradigms to medicinal applications. *Chem Soc Rev.* 2009;38:391–401.
116. Biot C, Glorian G, Maciejewski LA, Brocard JS, Domarle O, Blampain G, et al. Synthesis and antimalarial activity *in vitro* and *in vivo* of a new ferrocene-chloroquine analogue. *J Med Chem.* 1997;40:3715–8.
117. Wani WA, Jameel E, Baig U, Mumtazuddin S, Hun LT. Ferroquine and its derivatives: new generation of antimalarial agents. *Eur J Med Chem.* 2015;101:534–51.
118. Delhaes L, Biot C, Delcourt P, Maciejewski LA, Brocard S, Dive D. Synthesis of ferroquine enantiomers: first investigation of effects of metallocenic chirality upon antimalarial activity and cytotoxicity. *ChemBioChem.* 2002;3:418–23.
119. Chibale K, Moss JR, Blackie M, van Schalkwyk D, Smith PJ. New amine and urea analogs of ferrochloroquine: synthesis, antimalarial activity *in vitro* and electrochemical studies. *Tetrahedron Lett.* 2000;41:6231–5.
120. Beagley P, Blackie MAL, Chibale K, Clarkson C, Meijboom R, Moss JR, et al. Synthesis and antiplasmodial activity *in vitro* of new ferrocene-chloroquine analogues. *Dalton Trans.* 2003:3046–51.
121. Top S, Tang J, Vessières A, Carrez D, Provote C, Jaouen G. Ferrocenyl hydroxytamoxifen: a prototype for a new range of oestradiol receptor site-directed cytotoxics. *Chem Commun.* 1996:955–6.
122. Ferber B, Top S, Vessières A, Welter R, Jaouen G. Synthesis of optically pure *o*-formylcyclopentadienyl metal complexes of 17 α -ethynylestradiol. Recognition of the planar chirality by the estrogen receptor. *Organometallics.* 2006;25:5730–9.
123. Plazuk D, Top S, Vessières A, Plamont MA, Huché M, Zakrzewski J, et al. Organometallic cyclic polyphenols derived from 1,2-(α -keto tri or tetra methylene) ferrocene show strong antiproliferative activity on hormone-independent breast cancer cells. *Dalton Trans.* 2010;39:7444–50.
124. Cunningham L, Wang Y, Nottingham C, Pagsulingan J, Jaouen G, McGlinchey MJ, et al. Enantioselective synthesis of planar chiral ferrocenes that show chiral discrimination in antiproliferative activity on breast cancer cells. *ChemBioChem.* 2020;21:2974–81.
125. Baramee A, Coppin A, Mortuaire M, Pelinski L, Tomavo S, Brocard J. Synthesis and *in vitro* activities of ferrocenic aminohydroxynaphthoquinones against *Toxoplasma gondii* and *Plasmodium falciparum*. *Bioorg Med Chem.* 2006;14:1294–302.
126. Wambang N, Schifano-Faux N, Aillerie A, Baldeyrou B, Jacquet C, Bal-Mahieu C, et al. Synthesis and biological activity of ferrocenyl indeno[1,2-*c*]isoquinolines as topoisomerase II inhibitors. *Bioorg Med Chem.* 2016;24:651–60.
127. Bárány P, Szabó Oláh R, Kovács I, Czuczti T, Szabó CL, Takács A, et al. Ferrocene-containing imipridone (ONC201) hybrids: synthesis, DFT modelling, *in vitro* evaluation, and structure-activity relationships. *Molecules.* 2018;23:2248.
128. Mazur M, Mrozowicz M, Buchowicz W, Koszytkowska-Stawińska M, Kamiński R, Ochal Z, et al. Formylation of a metathesis-derived ansa[4]-ferrocene: a simple route to anticancer organometallics. *Dalton Trans.* 2020;49:11504–11.
129. Mazur M, Ziemkiewicz K, Rawiak K, Kisiel K, Wińska P, Deresz K, et al. *N*-Allyl-*N*-ferrocenylmethylamines and ansa-ferrocenylmethylamines: synthesis, structure, and biological evaluation. *Eur J Inorg Chem.* 2022;2022:e202101098.
130. Gong G, Cao Y, Wang F, Zhao G. Planar chiral ferrocene cyclopalladated derivatives induce caspase-dependent apoptosis and antimetastasis in cancer cells. *Organometallics.* 2018;37:1103–13.
131. Kedge JL, Nguyen HV, Khan Z, Male L, Ismail MK, Roberts HV, et al. Organometallic nucleoside analogues: effect of hydroxyalkyl linker length on cancer cell line toxicity. *Eur J Inorg Chem.* 2017;2017:466–76.
132. Wilde M, Arzur D, Baratte B, Lefebvre D, Robert T, Roisnel T, et al. Regorafenib analogues and their ferrocenic counterparts: synthesis and biological evaluation. *New J Chem.* 2020;44:19723–33.
133. Chuard T, Deschenaux R. Functional liquid-crystalline materials based on ferrocene. *Chimia.* 2003;57:597–600.
134. Brettar J, Bürgi T, Donnio B, Guillon D, Klappert R, Scharf T, et al. Ferrocene-containing optically active liquid-crystalline side-chain polysiloxanes with planar chirality. *Adv Funct Mat.* 2006;16:260–7.
135. Togni A, Rihs G. Synthesis and structure of enantiomerically pure ferrocene derivatives for nonlinear optics. *Organometallics.* 1993;12:3368–72.
136. Balavoine GGA, Daran J-C, Iftime G, Lacroix PG, Manoury E, Delaire JA, et al. Synthesis, crystal structures, and second-order nonlinear optical properties of new chiral ferrocenyl materials. *Organometallics.* 1999;18:21–9.
137. Roque K, Barangé F, Balavoine GGA, Daran J-C, Lacroix PG, Manoury E. New chiral ferrocenyl-pyridinium salts for non-linear optics. *J Organomet Chem.* 2001;637–639:531–7.
138. Mamane V, Ledoux-Rak I, Deveau S, Zyss J, Riant O. Palladium-catalyzed cross-coupling reaction of a chiral ferro-

- cenyl zinc reagent with aromatic bromides: application to the design of chiral octupoles for second harmonic generation. *Synthesis*. 2003;2003:455–67.
139. Srinivas P, Prabhakar S, Chevallier F, Nassar E, Erb W, Dorcet V, et al. Synthesis of ferrocene amides and esters from aminoferrocene and 2-substituted ferrocenecarboxylic acid and properties thereof. *New J Chem*. 2016;40:9441–7.
140. Alba AN, Rios R. Kinetic resolution: a powerful tool for the synthesis of planar-chiral ferrocenes. *Molecules*. 2009;14:4747–57.
141. Liu C-X, Gu Q, You S-L. Asymmetric C–H bond functionalization of ferrocenes: new opportunities and challenges. *Trends Chem*. 2020;2:737–49.
142. Wang Q, Nie Y-H, Liu C-X, Zhang W-W, Wu Z-J, Gu Q, et al. Rhodium(III)-catalyzed enantioselective C–H activation/annulation of ferrocenecarboxamides with internal alkynes. *ACS Catal*. 2022;12:3083–93.
143. Shibata T, Uno N, Sasaki T, Kanyiva KS. Pt-catalyzed enantioselective cycloisomerization for the synthesis of planar-chiral ferrocene derivatives. *J Org Chem*. 2016;81:6266–72.
144. Ito M, Okamura M, Kanyiva KS, Shibata T. Catalytic enantioselective synthesis of azepine-fused planar-chiral ferrocenes by Pt-catalyzed cycloisomerization. *Organometallics*. 2019;38:4029–35.
145. Zhang ZZ, Huang DY, Shi BF. Recent advances in the synthesis of ferrocene derivatives via 3d transition metal-catalyzed C–H functionalization. *Org Biomol Chem*. 2022;20:4061–73.
146. Mou Q, Zhao R, Niu R, Fukagawa S, Shigeno T, Yoshino T, et al. Cp*Ir(III)/chiral carboxylic acid-catalyzed enantioselective C–H alkylation of ferrocene carboxamides with diazomalones. *Org Chem Front*. 2021;8:6923–30.
147. Cao F, Chen Q, Shan H, Ling L, Hu J, Zhang H. Pd(II)-catalyzed azine-assisted enantioselective oxidative C–H/C–H cross-coupling of ferrocenes with various heteroarenes. *J Org Chem*. 2022;87:479–87.
148. Ruble JC, Fu GC. Chiral π -complexes of heterocycles with transition metals: a versatile new family of nucleophilic catalysts *J Org Chem*. 1996;61:7230–1.
149. Mamane V, Fort Y. Convenient access to new chiral ferrocene-(iso)quinolines. *J Org Chem*. 2005;70:8220–3.
150. Guthardt R, Blanckenberg J, Bruhn C, Siemeling U. Planar-chiral 1,1'-diaminoferrocenes. *Chem Commun*. 2021;57:12984–7.
151. Batsanov AS, Héroult D, Howard JAK, Patrick LGF, Probert MR, Whiting A. Synthesis and structure of planar chiral, bifunctional aminoboronic acid ferrocene derivatives. *Organometallics*. 2007;26:2414–9.
152. Datta A, Kollhofer A, Plenio H. Ir-catalyzed C–H activation in the synthesis of borylated ferrocenes and half sandwich compounds. *Chem Commun*. 2004:1508–9.
153. Tazi M, Erb W, Halauko YS, Ivashkevich OA, Matulis VE, Roisnel T, et al. From 2- to 3-substituted ferrocene carboxamides or how to apply halogen “dance” to the ferrocene series. *Organometallics*. 2017;36:4770–8.
154. Allouch F, Dwadnia N, Vologdin NV, Svyaschenko YV, Cattet H, Penouilh M-J, et al. Converging and diverging synthetic strategies to tetradentate (*N,N'*)-diaminomethyl, (*P,P'*)-ferrocenyl ligands: influence of *tert*-butyl groups on ferrocene backbone conformation. *Organometallics*. 2015;34:5015–28.
155. Lerayer E, Renaut P, Brandes S, Cattet H, Fleurat-Lessard P, Bouhadir G, et al. Planar-chiral 1,1'-diboryl metallocenes: diastereoselective synthesis from boryl cyclopentadienides and spin density analysis of a diborylcobaltocene. *Inorg Chem*. 2017;56:1966–73.
156. Lerayer E, Renaut P, Roger J, Pirio N, Cattet H, Fleurat-Lessard P, et al. A sterically congested 1,2-diphosphino-1'-boryl-ferrocene: synthesis, characterization and coordination to platinum. *Dalton Trans*. 2019;48:11191–5.
157. Fu GC. Applications of planar-chiral heterocycles as ligands in asymmetric catalysis. *Acc Chem Res*. 2006;39:853–60.
158. Lo MM-C, Fu GC. A new class of planar-chiral ligands: synthesis of a C_2 -symmetric bisazaferrocene and its application in the enantioselective Cu(I)-catalyzed cyclopropanation of olefins. *J Am Chem Soc*. 1998;120:10270–1.
159. Fukuda T, Imazato K, Iwao M. Enantioselective synthesis of planar chiral azaferrocenes via chiral ligand-mediated ring- and lateral-lithiations. *Tetrahedron Lett*. 2003;44:7503–6.
160. Anderson JC, Osborne JD, Woltering TJ. Enantioselective functionalisation of the C-2' position of 1,2,3,4,5-pentamethylazaferrocene via sparteine mediated lithiation: potential new ligands for asymmetric catalysis. *Org Biomol Chem*. 2008;6:330–9.
161. Hansen JG, Søtofte I, Johannsen M. An enantioselective synthesis of optically pure azaferrocenyl anion-first general and practical approach to chiral azaferrocenes. *Org Lett*. 2001;3:499–501.
162. Hansen JG, Johannsen M. Pentamethylated and pentaphenylated azaferro- and azaruthenocenes: simple and general methodology for the preparation of enantiopure derivatives. *J Org Chem*. 2003;68:1266–74.
163. Ogasawara M, Yoshida K, Hayashi T. Synthesis and characterization of a novel chiral phosphole and its derivatives. *Organometallics*. 2001;20:1014–9.
164. Ogasawara M, Ito A, Yoshida K, Hayashi T. Synthesis of 2,5-bis(binaphthyl)phospholes and phosphametallocene derivatives and their application in palladium-catalyzed asymmetric hydrosilylation. *Organometallics*. 2006;25:2715–8.
165. Ogasawara M, Watanabe S, Nakajima K, Takahashi T. Enantioselective synthesis of planar-chiral phosphoferrocenes by molybdenum-catalyzed asymmetric interannular ring-closing metathesis. *J Am Chem Soc*. 2010;132:2136–7.
166. Thomson JB. Molecular asymmetry in the ferrocene series. *Tetrahedron Lett*. 1959;6:26–7.
167. Falk H, Fröstl W, Schlögl K. Darstellung, chiroptische Eigenschaften und absolute Konfiguration von 7.7'-Spiro-bi[3]ferrocenophan-6.6'-dion. *Monatsh Chem*. 1971;102:1270–8.
168. Schlögl KA, Widhalm M. Recycling technique for the chromatographic separation of enantiomers and diastereomers on triacetylcellulose. *Monatsh Chem*. 1984;115:1113–20.
169. Trainor G, Breslow R. High acylation rates and enantioselectivity with cyclodextrin complexes of rigid substrates. *J Am Chem Soc*. 1981;103:154–8.
170. Breslow R, Trainor G, Ueno A. Optimization of metallocene substrates for β -cyclodextrin reactions. *J Am Chem Soc*. 1983;105:2739–44.

171. Le Noble WJ, Srivastava S, Breslow R, Trainor G. Effect of pressure on two cyclodextrin-promoted ester hydrolyses. *J Am Chem Soc.* 1983;105:2745–8.
172. Harada A, Takahashi S. Preparation and properties of cyclodextrin-ferrocene inclusion complexes. *J Chem Soc Chem Commun.* 1984:645–6.
173. Chen XP, Zhou ZM, Yuan H, Meng ZH. Preparation and chiral recognition of a novel chiral stationary phase for HPLC, based on mono(6^A-N-1-(2-hydroxy)phenylethylimino-6^A-deoxy)- β -cyclodextrin and covalently bonded silica gel. *Chin Chem Lett.* 2008;19:797–800.
174. Chen X, Zhou Z, Yuan H, Meng Z. Preparation and chiral recognition of a mono[6^A-N-1-(2-hydroxy)-phenylethylimino-6^A-deoxy]- β -cyclodextrin HPLC stationary phase. *J Chromatogr Sci.* 2008;46:777–82.
175. Zhou ZM, Li X, Chen XP, Fang M, Dong X. Separation performance and recognition mechanism of mono(6-deoxy-imino)- β -cyclodextrins chiral stationary phases in high-performance liquid chromatography. *Talanta.* 2010;82:775–84.
176. Snegur LV, Borisov YA, Ermolenko YV, Safronova VN, Kiselev SS, Kochetkov KA, et al. Application of capillary electrophoresis technique for the enantioseparation of bioactive ferrocene-based compounds versus DFT calculated data. *Electrophoresis.* 2020;41:1969–79.
177. Yamazaki Y, Uebayasi M, Hosono K. Enantiotopic differentiation in horse-liver alcohol-dehydrogenase-catalyzed oxidoreduction studied with novel substrates having organometallic moieties. *Eur J Biochem.* 1989;184:671–80.
178. Yamazaki Y, Morohashi N, Hosono H. High-performance liquid chromatographic determination of optical purity of planar chiral organometallic compounds resolved by enzymic transformations. *J Chromatogr A.* 1991;542:129–36.
179. Dosa PI, Ruble JC, Fu GC. Planar-chiral heterocycles as ligands in metal-catalyzed processes: enantioselective addition of organozinc reagents to aldehydes. *J Org Chem.* 1997;62:444–5.
180. Qiao S, Fu GC. The first application of a planar-chiral phosphorus heterocycle in asymmetric catalysis: enantioselective hydrogenation of dehydroamino acids. *J Org Chem.* 1998;63:4168–9.
181. Rios R, Liang J, Lo MM-C, Fu GC. Synthesis, resolution and crystallographic characterization of a new C₂-symmetric planar-chiral bipyridine ligand: application to the catalytic enantioselective cyclopropanation of olefins. *Chem Commun.* 2000;377–8.
182. Peluso P, Mamane V, Dallochio R, Dessi A, Cossu S. Noncovalent interactions in high-performance liquid chromatography enantioseparations on polysaccharide-based chiral selectors. *J Chromatogr A.* 2020;1623:461202.
183. Peluso P, Mamane V, Dessi A, Dallochio R, Aubert E, Gatti C, et al. Halogen bond in separation science: a critical analysis across experimental and theoretical results. *J Chromatogr A.* 2020;1616:460788.
184. Metallinos C, Szillat H, Taylor NJ, Snieckus V. (-)-Sparteine-mediated directed *ortho*-metalation of *N*-cumyl-*N*-ethylferrocenecarboxamide. Versatile routes to functionalized planar chiral ferrocenecarboxamides, amines, esters and phosphines. *Adv Synth Cat.* 2003;345:370–82.
185. Patti A, Pedotti S. Parallel or classical kinetic resolution of a planar chiral ferrocenyketone through asymmetric reductions. *Tetrahedron: Asymmetry.* 2010;21:2631–7.
186. Riant O, Argouarch G, Guillauneux D, Samuel O, Kagan HB. A straightforward asymmetric synthesis of enantiopure 1,2-disubstituted ferrocenes. *J Org Chem.* 1998;63:3511–4.
187. Dai X, Nakai T, Romero JA, Fu GC. Enantioselective synthesis of protected amines by the catalytic asymmetric addition of hydrazoic acid to ketenes. *Angew Chem Int Ed.* 2007;46:4367–9.
188. Ruble JC, Fu GC. Enantioselective construction of quaternary stereocenters: rearrangements of *O*-acylated azlactones catalyzed by a planar-chiral derivative of 4-(pyrrolidino)pyridine. *J Am Chem Soc.* 1998;120:11532–3.
189. Sudhakar A, Katz TJ. Asymmetric synthesis of helical metallocenes. *J Am Chem Soc.* 1986;108:179–81.
190. Akiyama M, Nozaki K. Synthesis of optically pure helicene metallocenes. *Angew Chem Int Ed.* 2017;56:2040–4.
191. Urbano A, Hernandez-Torres G, Del Hoyo AM, Martinez-Carrion A, Carmen Carreno M. Mild access to planar-chiral ortho-condensed aromatic ferrocenes via gold(I)-catalyzed cycloisomerization of ortho-alkynylaryl ferrocenes. *Chem Commun.* 2016;52:6419–22.
192. Tribedi S, Kitaura K, Nakajima T, Sunoj RB. On the question of steric repulsion versus noncovalent attractive interactions in chiral phosphoric acid catalyzed asymmetric reactions. *Phys Chem Chem Phys.* 2021;23:18936–50.
193. Thorat RA, Jain S, Sattar M, Yadav P, Mandhar Y, Kumar S. Synthesis of chiral-substituted 2-aryl-ferrocenes by the Catellani reaction. *J Org Chem.* 2020;85:14866–78.
194. Butenschön H. Haloferrocenes: syntheses and selected reactions. *Synthesis.* 2018;50:3787–808.
195. Wen M, Erb W, Mongin F, Halauko YS, Ivashkevich OA, Matulis VE, et al. Synthesis of polysubstituted ferrocenesulfoxides. *Molecules.* 2022;27:1798.
196. Erb W, Carré V, Roisnel T. HFIP-promoted substitution in the ferrocene series: smooth approach towards original catalysts. *Eur J Org Chem.* 2021;2021:5702–16.
197. Ogasawara M, Enomoto Y, Uryu M, Yang X, Kataoka A, Ohnishi A. Application of polysaccharide-based chiral HPLC columns for separation of nonenantiomeric isomeric mixtures of organometallic compounds. *Organometallics.* 2019;38:512–8.
198. Morvan A, Garnier C, Furman C, Speybrouck D, Boulanger E, Ghinet A, et al. Separation of planar chiral ferrocenes by capillary electrokinetic chromatography and liquid chromatography. *J Chromatogr A.* 2022;1677:463306.

SUPPORTING INFORMATION

Additional supporting information can be found online in the Supporting Information section at the end of this article.

How to cite this article: Peluso P, Mamane V. Ferrocene derivatives with planar chirality and their enantioseparation by liquid-phase techniques. *Electrophoresis.* 2022;1–32.
<https://doi.org/10.1002/elps.202200148>